Table 1. Allele and genotype frequencies of SNP in *DGKH, DFNB31* and *SORCS2* in the case–control sample

Gene	SNP ID		HWE *P*-value	*n*	Allele		*P*-value (Fisher's exact test)	Genotype			*P*-value (Fisher's exact test)	MAF
DGKH					T	C		T/T	T/C	C/C		
	rs9315885	BD	0.5045	364	333	395		73	187	104		45.7%
		CT	0.9530	370	336	404	0.9166	76	184	110	0.9094	45.4%
					A	C		A/A	A/C	C/C		
	rs1012053	BD	0.4608	364	359	369		85	189	90		49.3%
		CT	0.9595	369	366	372	0.9169	91	184	94	0.8578	49.6%
					A	G		A/A	A/G	G/G		
	rs1170195	BD	0.2023	360	352	368		80	192	88		51.1%
		CT	0.7547	370	372	368	0.6011	92	188	90	0.6789	49.7%
					T	C		T/T	T/C	C/C		
	rs9525570	BD	0.7813	360	615	105		262	91	7		14.6%
		CT	0.7634	368	645	91	0.2201	282	81	5	0.4520	12.4%
					C	T		C/C	C/T	T/T		
	rs1170191	BD	0.2748	358	373	343		92	189	77		47.9%
		CT	0.9982	368	364	372	0.3190	90	184	94	0.4430	50.5%
					T	C		T/T	T/C	C/C		
	rs9315897	BD	0.8558	364	623	105		267	89	8		14.4%
		CT	0.6845	369	645	93	0.3211	281	83	5	0.5399	12.6%
					C	T		C/C	C/T	T/T		
	rs35776153†	BD	N/A	365	730	0		365	0	0		0.0%
		CT	N/A	370	740	0	1.0000	370	0	0	1.0000	0.0%
					T	C		T/T	T/C	C/C		
	rs17646069†	BD	0.5476	365	634	96		274	86	5		13.2%
		CT	0.0858	370	632	108	0.4508	274	84	12	0.2630	14.6%
DFNB31					T	G		T/T	T/G	G/G		
	rs2274158†	BD	0.8790	362	283	441		56	171	135		39.1%
		CT	0.5230	369	305	433	0.3937	66	173	130	0.6525	41.3%
					A	G		A/A	A/G	G/G		
	rs2274159†	BD	0.4654	364	336	392		81	174	109		46.2%
		CT	0.9039	369	347	391	0.7536	81	185	103	0.7906	47.0%
					A	G		A/A	A/G	G/G		
	rs942519†	BD	0.5699	364	320	408		73	174	117		44.0%
		CT	0.8110	370	329	411	0.8747	72	185	113	0.8363	44.5%
					T	C		T/T	T/C	C/C		
	rs4978584†	BD	0.9308	365	290	440		58	174	133		39.7%
		CT	0.4675	370	302	438	0.7097	65	172	133	0.8363	40.8%
					C	G		C/C	C/G	G/G		
	rs35003670†	BD	N/A	362	724	0		362	0	0		0.0%
		CT	N/A	370	740	0	1.0000	370	0	0	1.0000	0.0%
					A	G		A/A	A/G	G/G		
	rs942518	BP	0.2645	363	563	163		222	119	22		22.5%
		CT	0.4526	370	561	179	0.4587	210	141	19	0.3087	24.2%
SORCS2					T	C		T/T	T/C	C/C		
	rs4411993	BD	0.8482	360	227	493		35	157	168		31.5%
		CT	0.2895	367	221	513	0.5703	29	163	175	0.6969	30.1%
					G	C		G/G	G/C	C/C		
	rs11736984‡	BP	0.2064	364	192	536		30	132	202		26.4%
		CT	0.1696	369	184	554	0.5499	18	148	203	0.1457	24.9%

Table 1. (*Continued*)

Gene	SNP ID		HWE *P*-value	*n*	Allele		*P*-value (Fisher's exact test)	Genotype			*P*-value (Fisher's exact test)	MAF
					T	C		T/T	T/C	C/C		
	rs10937823	BD	0.0500	363	200	526		35	130	198		27.5%
		CT	0.0681	370	187	553	0.3432	17	153	200	0.0175*	25.3%
					G	C		G/G	G/C	C/C		
	rs13139074‡	BP	0.4360	366	206	526		32	142	192		28.1%
		CT	0.3993	367	188	546	0.2891	21	146	200	0.2929	25.6%
					A	G		A/A	A/G	G/G		
	rs11734984‡	BP	0.4737	363	206	520		32	142	189		28.4%
		CT	0.8256	370	203	537	0.7268	27	149	194	0.7501	27.4%
					T	C		T/T	T/C	C/C		
	rs12645507‡	BP	0.0801	365	449	281		146	157	62		38.5%
		CT	0.9372	368	472	264	0.3049	151	170	47	0.2682	35.9%
					G	A		G/G	G/A	A/A		
	rs34058821†	BD	N/A	366	732	0		366	0	0		0.0%
		CT	N/A	369	738	0	1.0000	369	0	0	1.0000	0.0%
					T	C		T/T	T/C	C/C		
	rs16840892†	BD	0.0254	364	254	474		54	146	164		34.9%
		CT	0.2437	370	255	485	0.8695	49	157	164	0.7480	34.5%

*$P < 0.05$.
†Non-synonymous SNP.
‡Additionally examined SNP.
BD, bipolar disorder sample; CT, control sample; HWE, Hardy–Weinberg equilibrium; MAF, minor allele frequency; *n*, number of genotyped participants; SNP, single-nucleotide polymorphism.

Table 2. Result of the meta-analysis of four SNP in *DGKH*

	Present study				Zeng *et al.*[21]				Meta-analysis	
	MAF†				MAF†					
SNP, minor allele†	Cases ($n = 366$)	Controls ($n = 370$)	*P*	OR (95%CI)	Cases ($n = 1139$)	Controls ($n = 1138$)	*P*	OR (95%CI)	*P*	OR (95%CI)
rs9315885, T	0.457	0.454	0.9166	1.01 (0.83,1.24)	0.493	0.482	0.453	1.04 (0.93,1.17)	0.478‡	1.04 (0.94,1.15)
rs1012053, A	0.493	0.496	0.9169	0.99 (0.81,1.21)	0.527	0.507	0.191	1.08 (0.97,1.22)	0.258‡	1.06 (0.96,1.17)
rs1170191, C	0.521	0.495	0.3190	1.11 (0.90,1.37)	0.528	0.508	0.179	1.08 (0.97,1.22)	0.093‡	1.09 (0.99,1.21)
rs9315897, C	0.144	0.126	0.3211	1.17 (0.87,1.58)	0.111	0.095	0.089	1.19 (0.98,1.44)	0.039*‡	1.18 (1.01,1.39)

*$P < 0.05$.
†Minor alleles in the Japanese control samples.
‡Test for heterogeneity: $I^2 = 0\%$.
CI, confidence interval; MAF, minor allele frequency; OR, odds ratio; SNP, single-nucleotide polymorphism.

ACKNOWLEDGMENTS

This study was supported in part by Health and Labour Sciences Research Grants (Research on Psychiatric and Neurological Diseases and Mental Health [2006–012] Neurophysiology, neuroimaging, and molecular biology of bipolar disorders).

REFERENCES

1. Taylor L, Faraone SV, Tsuang MT. Family, twin, and adoption studies of bipolar disease. *Curr. Psychiatry Rep.* 2002; **4**: 130–133.
2. Baum AE, Akula N, Cabanero M *et al.* A genome-wide association study implicates diacylglycerol kinase eta (DGKH) and several other genes in the etiology of bipolar disorder. *Mol. Psychiatry* 2008; **13**: 197–207.
3. Ferreira MA, O'Donovan MC, Meng YA *et al.* Collaborative genome-wide association analysis supports a role for ANK3 and CACNA1C in bipolar disorder. *Nat. Genet.* 2008; **40**: 1056–1058.
4. Sklar P, Smoller JW, Fan J *et al.* Whole-genome association study of bipolar disorder. *Mol. Psychiatry* 2008; **13**: 558–569.
5. Smith EN, Bloss CS, Badner JA *et al.* Genome-wide association study of bipolar disorder in European American and African American individuals. *Mol. Psychiatry* 2009; **14**: 755–763.
6. WTCCC. Genome-wide association study of 14,000 cases of seven common diseases and 3,000 shared controls. *Nature* 2007; **447**: 661–678.
7. Lee MT, Chen CH, Lee CS *et al.* Genome-wide association study of bipolar I disorder in the Han Chinese population. *Mol. Psychiatry* 2010 (in press).
8. McMahon FJ, Akula N, Schulze TG *et al.* Meta-analysis of genome-wide association data identifies a risk locus for major mood disorders on 3p21.1. *Nat. Genet.* 2010; **42**: 128–131.
9. Liu Y, Blackwood DH, Caesar S *et al.* Meta-analysis of genome-wide association data of bipolar disorder and major depressive disorder. *Mol. Psychiatry* 2011; **16**: 2–4.
10. Berridge MJ. The Albert Lasker Medical Awards. Inositol trisphosphate, calcium, lithium, and cell signaling. *JAMA* 1989; **262**: 1834–1841.
11. Yap CC, Liang F, Yamazaki Y *et al.* CIP98, a novel PDZ domain protein, is expressed in the central nervous system and interacts with calmodulin-dependent serine kinase. *J. Neurochem.* 2003; **85**: 123–134.
12. Mburu P, Mustapha M, Varela A *et al.* Defects in whirlin, a PDZ domain molecule involved in stereocilia elongation, cause deafness in the whirler mouse and families with DFNB31. *Nat. Genet.* 2003; **34**: 421–428.
13. Tamayo ML, Maldonado C, Plaza SL *et al.* Neuroradiology and clinical aspects of Usher syndrome. *Clin. Genet.* 1996; **50**: 126–132.
14. Hermey G, Plath N, Hubner CA, Kuhl D, Schaller HC, Hermans-Borgmeyer I. The three sorCS genes are differentially expressed and regulated by synaptic activity. *J. Neurochem.* 2004; **88**: 1470–1476.
15. Hermey G. The Vps10p-domain receptor family. *Cell. Mol. Life Sci.* 2009; **66**: 2677–2689.
16. Scott LJ, Muglia P, Kong XQ *et al.* Genome-wide association and meta-analysis of bipolar disorder in individuals of European ancestry. *Proc. Natl. Acad. Sci. USA* 2009; **106**: 7501–7506.
17. Hattori E, Toyota T, Ishitsuka Y *et al.* Preliminary genome-wide association study of bipolar disorder in the Japanese population. *Am. J. Med. Genet. B Neuropsychiatr. Genet.* 2009; **150B**: 1110–1117.
18. Squassina A, Manchia M, Congiu D *et al.* The diacylglycerol kinase eta gene and bipolar disorder: a replication study in a Sardinian sample. *Mol. Psychiatry* 2009; **14**: 350–351.
19. Tesli M, Kahler AK, Andreassen BK *et al.* No association between DGKH and bipolar disorder in a Scandinavian case-control sample. *Psychiatr. Genet.* 2009; **19**: 269–272.
20. Ollila HM, Soronen P, Silander K *et al.* Findings from bipolar disorder genome-wide association studies replicate in a Finnish bipolar family-cohort. *Mol. Psychiatry* 2009; **14**: 351–353.
21. Zeng Z, Wang T, Li T *et al.* Common SNPs and haplotypes in DGKH are associated with bipolar disorder and schizophrenia in the Chinese Han population. *Mol. Psychiatry* 2010 (in press).
22. Barrett JC, Fry B, Maller J, Daly MJ. Haploview: analysis and visualization of LD and haplotype maps. *Bioinformatics* 2005; **21**: 263–265.
23. *Review Manager (RevMan)* [Computer program]. Version 5.0. The Nordic Cochrane Centre, The Cochrane Collaboration, Copenhagen, 2008.
24. Higgins JP, Thompson SG. Controlling the risk of spurious findings from meta-regression. *Stat. Med.* 2004; **23**: 1663–1682.
25. Trikalinos TA, Salanti G, Zintzaras E, Ioannidis JP. Meta-analysis methods. *Adv. Genet.* 2008; **60**: 311–334.
26. Xu Z, Taylor JA. SNPinfo: integrating GWAS and candidate gene information into functional SNP selection for genetic association studies. *Nucleic Acids Res.* 2009; **37**: W600–W605.
27. Spencer CC, Su Z, Donnelly P, Marchini J. Designing genome-wide association studies: sample size, power, imputation, and the choice of genotyping chip. *PLoS Genet.* 2009; **5**: e1000477.
28. Purcell S, Cherny SS, Sham PC. Genetic Power Calculator: design of linkage and association genetic mapping studies of complex traits. *Bioinformatics* 2003; **19**: 149–150.
29. Yamaguchi-Kabata Y, Nakazono K, Takahashi A *et al.* Japanese population structure, based on SNP genotypes from 7003 individuals compared to other ethnic groups: effects on population-based association studies. *Am. J. Hum. Genet.* 2008; **83**: 445–456.

Schizophrenia Research 129 (2011) 172–182

Contents lists available at ScienceDirect

Schizophrenia Research

journal homepage: www.elsevier.com/locate/schres

Aripiprazole inhibits superoxide generation from phorbol-myristate-acetate (PMA)-stimulated microglia in vitro: Implication for antioxidative psychotropic actions via microglia

Takahiro A. Kato [a,b,*], Akira Monji [a,*], Keiji Yasukawa [b,c], Yoshito Mizoguchi [a], Hideki Horikawa [a], Yoshihiro Seki [a], Sadayuki Hashioka [a], Youn-Hee Han [c,d], Mina Kasai [a], Noriyuki Sonoda [b,e], Eiichi Hirata [b,e], Yasutaka Maeda [b,e], Toyoshi Inoguchi [b,e], Hideo Utsumi [b], Shigenobu Kanba [a]

[a] Department of Neuropsychiatry, Graduate School of Medical Sciences, Kyushu University, Maidashi 3-1-1; Higashi-ku, Fukuoka 812-8582, Japan
[b] Innovation Center for Medical Redox Navigation, Kyushu University, Maidashi 3-1-1, Higashi-ku, Fukuoka 812-8582, Japan
[c] Department of Chemo-Pharmaceutical Sciences, Graduate School of Pharmaceutical Sciences, Kyushu University, 3-1-1 Maidashi Higashi-ku, Fukuoka 812-8582, Japan
[d] Department of Civil and Environmental Engineering, Tohoku Gakuin University, 1-13-1 Chou, Tagajo, 985-8537, Japan
[e] Department of Internal Medicine and Bioregulatory Science, Graduate School of Medical Sciences, Kyushu University, Maidashi 3-1-1, Higashi-ku, Fukuoka 812-8582, Japan

ARTICLE INFO

Article history:
Received 1 October 2010
Received in revised form 20 March 2011
Accepted 21 March 2011
Available online 15 April 2011

Keywords:
Microglia
Schizophrenia
Oxidative stress
Antipsychotics
Superoxide
NADPH oxidase

ABSTRACT

Altered antioxidant status has been implicated in schizophrenia. Microglia, major sources of free radicals such as superoxide ($\bullet O_2^-$), play crucial roles in various brain pathologies. Recent postmortem and imaging studies have indicated microglial activation in the brain of schizophrenic patients. We previously demonstrated that atypical antipsychotics including aripiprazole significantly inhibited the release of nitric oxide and proinflammatory cytokines from interferon-γ-stimulated microglia in vitro. Antioxidative effects of antipsychotics via modulating microglial superoxide generation have never been reported. Therefore, we herein investigated the effects of antipsychotics on the $\bullet O_2^-$ generation from phorbol-myristate-acetate (PMA)-stimulated rodent microglia by the electron spin resonance (ESR) spectroscopy and also examined the intracellular mechanism by intracellular Ca^{2+} imaging and immunostaining. Neuronal damage induced by microglial activation was also investigated by the co-culture experiment.

Among various antipsychotics, only aripiprazole inhibited the $\bullet O_2^-$ generation from PMA-stimulated microglia. Aripiprazole proved to inhibit the $\bullet O_2^-$ generation through the cascade of protein kinase C (PKC) activation, intracellular Ca^{2+} regulation and NADPH oxidase activation via cytosolic $p47^{phox}$ translocation to the plasma/phagosomal membranes. Formation of neuritic beading, induced by PMA-stimulated microglia, was attenuated by pretreatment of aripiprazole.

D2R antagonism has long been considered as the primary therapeutic action for schizophrenia. Aripiprazole with D2R partial agonism is effective like other antipsychotics with fewer side effects, while aripiprazole's therapeutic mechanism itself remains unclear. Our results imply that aripiprazole may have psychotropic effects by reducing the microglial oxidative reactions and following neuronal reactions, which puts forward a novel therapeutic hypothesis in schizophrenia research.

1. Introduction

Altered antioxidant status has recently been implicated in schizophrenia with increasing number of clinical evidence measuring biochemical components for detoxification of reactive oxygen species (ROS) such as glutathione (GSH) and superoxide dismutase (SOD) (Do et al., 2009; Ng et al., 2008; Yao et al., 2001; Zhang et al., 2009a). A recent postmortem study and a cerebral spectroscopic study indicated a positive relationship between oxidative stress and schizophrenia (Treasaden and Puri, 2008; Wang et al., 2009). Overproduction of neutrophil ROS has reported to correlate with negative symptoms in schizophrenia (Sirota et al., 2003). Ketamine, which can lead to a syndrome indistinguishable from schizophrenia, has recently been

Abbreviations: DMSO, dimethyl sulfoxide; DPI, diphenylene iodonium; D2R, dopamine D2 receptor; ESR, electron spin resonance; GSH, glutathione; GM-CSF, granulocyte macrophage colony stimulating factor; $[Ca^{2+}]i$, intracellular Ca^{2+} concentration; NAC, N-Acetyl cysteine; NGF, nerve growth factor; NO, nitric oxide; PKC, protein kinase C; ROS, reactive oxygen species; $\bullet O_2^-$, superoxide; SOD, superoxide dismutase; TNF-α, tumor necrosis factor-α.

* Corresponding authors at: Department of Neuropsychiatry, Graduate School of Medical Sciences, Kyushu University, Maidashi 3-1-1, Higashi-ku, Fukuoka 812-8582, Japan. Tel.: +81 92 642 5627; fax: +81 92 642 5644.
E-mail addresses: takahiro@npsych.med.kyushu-u.ac.jp (T.A. Kato), amonji@hf.rim.or.jp (A. Monji).

0920-9964/$ – see front matter © 2011 Elsevier B.V. All rights reserved.
doi:10.1016/j.schres.2011.03.019

reported to induce a persistent increase in brain superoxide radicals due to activation of NADPH oxidase (Behrens et al., 2007). On the other hand, N-Acetyl cysteine (NAC), a glutathione precursor, has recently been reported to be effective for augmentation therapy of chronic schizophrenia and to improve impaired mismatch negativity in schizophrenic patients (Berk et al., 2008; Lavoie et al., 2008). More recently, the serum levels of SOD in chronic patients with schizophrenia are associated with psychopathology and response to antipsychotics (Zhang et al., 2009b). These findings suggest that regulation of oxidative stress may be related to the pathophysiology and therapeutic mechanism of schizophrenia.

Microglia, major sources of free radicals such as superoxide ($\bullet O_2^-$) and nitric oxide (NO) in the CNS, play a crucial role in variety of brain pathologies (Block and Hong, 2005; Block et al., 2007; Hanisch and Kettenmann, 2007). The pathophysiology of schizophrenia remains unclear, while recent postmortem brain studies using class II human leucocyte antigen (HLA-DR) have revealed microglial activation in the brains of schizophrenic patients (Radewicz et al., 2000; Steiner et al., 2008). Positron emission computed tomography (PET) studies with specific ligand of the peripheral benzodiazepine-binding sites (PBBS), have indicated that activated microglia may be present in schizophrenic patients (Doorduin et al., 2009; Takano et al., 2010; van Berckel et al., 2008). There is accumulated evidence that gene–environmental interaction via various factors such as virus infections and social stress leads to development of schizophrenia (Dalman et al., 2008; Jia et al., 2010; Mortensen et al., 2010; van Winkel et al., 2008). Microglia is one of the key players in brain damages induced by virus infections in the CNS (Block et al., 2007). One recent experiment suggested that social stress – isolation – induces NADPH oxidase activation via microglia in rat brain (Schiavone et al., 2009). These reports indicate that microglia may play an important role in gene–environmental interaction associated with schizophrenia (Sawa et al., 2004; Seshadri et al., 2010).

Dopamine system dysfunction has been for long time hypothesized in the pathology of schizophrenia, and dopamine D2 receptor (D2R) antagonism against dopamine neurons has been considered as the primary therapeutic target for schizophrenia (Kapur and Mamo, 2003; Miyamoto et al., 2005). On the other hand, aripiprazole is a novel unique atypical antipsychotic drug, which is a high-affinity D2R partial agonist (Burris et al., 2002; Shapiro et al., 2003). In spite of its different pharmacological profile, aripiprazole is effective against the positive and negative symptoms of patients with schizophrenia like other antipsychotics with fewer side effects (Leucht et al., 2009; Potkin et al., 2003).

We recently demonstrated that not only atypical antipsychotics with D2R antagonism but also aripiprazole with D2R partial agonism significantly inhibited the release of NO and proinflammatory cytokines such as tumor necrosis factor (TNF)-α on interferon-γ-stimulated microglia in vitro (Bian et al., 2008; Kato et al., 2008; Kato et al., 2007). Therapeutic benefits on psychotic symptoms have been demonstrated by COX-2 inhibitor and minocycline, both of which have proved to inhibit microglial activation (Akhondzadeh et al., 2007; Miyaoka et al., 2008; Muller et al., 2010). Summing up the above-mentioned evidence, we hypothesis that microglia may play a key role in the pathophysiology of schizophrenia by producing free radicals and cytokines in the CNS, and that microglial regulation may be a novel therapeutic target for schizophrenia (Monji et al., 2009).

To the best of our knowledge, antioxidative effects of antipsychotics via modulating microglial superoxide generation have never been reported. Phorbol-myristate-acetate (PMA), a typical activator of protein kinase C (PKC), induces $\bullet O_2^-$ from microglia with the elevation of intracellular calcium (Colton et al., 1992; Sankarapandi et al., 1998; Yoo et al., 1996). PKC has recently been indicated to be associated with stress-related illness and psychiatric disorders (Chen et al., 2009; Hains et al., 2009). Therefore, in the present study, we investigated the effects of various antipsychotics on the generation of $\bullet O_2^-$ from PMA-stimulated microglia by the electron spin resonance (ESR) spectroscopy and also examined the intracellular mechanism by intracellular Ca^{2+} imaging and immunostaining. Neuronal damage induced by microglial activation was also investigated by co-culture experiment.

2. Materials and methods

2.1. Chemicals and reagents

PMA was purchased from Biomol International (Plymouth Meeting, PA, USA). LPS, haloperidol, clozapine, a D2R full agonist; quinpirole, NADPH oxidase inhibitors; diphenylene iodonium (DPI) and apocynin, and a spin trap; DEPMPO were purchased from Sigma Chemicals (St. Louis, MO, USA). SOD, catalase, xanthine, and xanthine oxidase were purchased from Wako Pure Chemical Industries (Osaka, Japan). Recombinant mouse GM-CSF was purchased from R&D systems (Minneapolis, MN, USA). WST-8 was purchased from Dojindo Molecular Technologies (Kumamoto, Japan). Atypical antipsychotics were generously provided by each manufacturer; aripiprazole from Otsuka Pharmaceutical Co., Ltd. (Tokyo, Japan), risperidone from Janssen Pharmaceutica NV (Beerse, Belgium), and olanzapine from Eli Lilly and Co. (Indianapolis, IN, USA). Antipsychotics were dissolved initially into 20 mM with dimethyl sulfoxide (DMSO) and then were diluted into final concentration for each experiment. The final concentrations of antipsychotics were not over 10 μM. All antipsychotics and DMSO at the highest concentration (0.05%) were confirmed not to be toxic to microglial cells in our previous reports (Kato et al., 2007, 2008).

2.2. Cell cultures

All experimental procedures were conducted in accordance with the Standard Guidelines for Animal Experiments of Kyushu University. Rat primary microglial cells were cultured as previously described (Kato et al., 2008; Seki et al., 2010). Briefly, primary mixed cells were prepared from the whole brain of the 3-day-postnatal Sprague–Dawley rats, using Cell Strainer (BD Falcon, Franklin Lakes, NJ). Primary rat microglial cells were selected after attachment to Aclar film (Nisshin EM, Tokyo, Japan) for 2 h in Dulbecco's Modified Eagle's Medium supplemented with 10% fetal bovine serum (10% FBS/DMEM). Aclar films were slightly washed by PBS and then transferred to fresh 10% FBS/DMEM, and the fresh microglia was expanded for 1–2 days. The purity of the isolated microglia was assessed by immunocytochemical staining for microglial marker, Iba-1, and >99% of cells were stained positively. Murine microglial 6-3 cells, which was established from neonatal C57BL/6J(H-2b) mice using a non-enzymatic and non-virus-transformed procedure and which closely resemble primary cultured microglia (Kanzawa et al., 2000; Sawada et al., 1998), were cultured as previously described (Bian et al., 2008; Kato et al., 2007). The rat pheochromocytoma PC12 cells were cultured as previously described (Bian et al., 2008). Briefly, the 6-3 cells and PC12 cells were cultured in Eagle's minimal essential medium, 0.3% $NaHCO_3$, 2 mM glutamine, 0.2% glucose, 10 g/mL insulin and 10% fetal calf serum, and then were maintained at 37 °C in a 5% CO_2 and 95% air atmosphere.

2.3. Measurements of superoxide production

2.3.1. Electron spin resonance (ESR) spectroscopy

ESR, together with the spin-trapping agent DEPMPO was employed to accurately detect the production of $\bullet O_2^-$ from PMA-stimulated microglia. We previously described the detail methodology of the ESR (Hashioka et al., 2007a, 2007b). Briefly, the 6-3 cells were cultured on 12-well tissue plates at the density of 1.6×10^6 cells in 400 mL of serum-free medium per well. The 6-3 cells were incubated with 400 ng/mL PMA for 30 min in both the presence and absence of pretreatment of the antipsychotics for 5 h at 37 °C before beginning the detection of ESR spectra. Cell suspensions (4×10^6 cells/

mL) in the culture medium containing 25 mM DEPMPO were transferred to a standard cell capillary, and the ESR measurements were performed at room temperature right after the incubation. The ESR spectra were obtained using a JES-RE1X ESR spectrometer (JEOL, Japan). The setting conditions of the instrument were as follows: magnetic field = 336.7 + 7.5 mT, modulation amplitude = 2000, modulation width = 0.1 mT, modulation frequency = 100 kHz, time constant = 0.1 s, microwave power = 10 mW, microwave frequency = 9430 MHz, and sweep time = 2 min.

ESR was also applied to the rat primary microglial cells. The cells were cultured on 12-well tissue plates at a much lower density of 1.6×10^4 cells in 400 mL of serum-free culture medium per well due to the difficulty in collecting these cells.

2.3.2. Nitro blue tetrazolium (NBT) assay

The quantification of $\bullet O_2^-$ production in microglial cells was performed with modification of Nitro blue tetrazolium (NBT) assay as previously reported (Choi et al., 2006; Tan and Berridge, 2000). As a water-soluble formazan dye, we used the WST-8 (2-(2-methoxy-4-nitrophenyl)-3-(4-nitrophenyl)-5-(2,4-disulfophenyl)-2H-tetrazolium monosodium salt; Dojindo, Kumamoto, Japan). Briefly, microglial cells grown on 96-well culture plates (5×10^3 cells per well) were pre-incubated in the presence and absence of aripiprazole for 5 h and then the medium was changed to 50 μL chelated medium both in the presence and absence of 50 U/mL SOD at 37 °C. After 30 min of incubation with PMA (400 ng/mL), the supernatants were mixed with 5 μL WST-8 solution. The absorbance was read at 450 nm using a plate reader (Labsystems Multiscan MS). The comparative volumes of $\bullet O_2^-$ production were determined by the difference between the absorbance with SOD and that without SOD.

2.4. Spin trapping in xanthine/xanthine oxidase system

Xanthine oxidase (0.1 U/mL) was incubated with 0.4 mM xanthine in phosphate-buffer (PB) containing 2 mM DTPA and 20 mM DEPMPO in the presence and absence of aripiprazole. Xanthine oxidase was added last to the mixture to start the reaction. The ESR spectra were recorded at room temperature on a JES-RE1X ESR spectrometer. The setting conditions of the instrument were as follows: magnetic field = 336.7 + 7.5 mT, modulation amplitude = 500, modulation width = 0.1 mT, modulation frequency = 100 kHz, time constant = 0.03 s, microwave power = 10 mW, microwave frequency = 9430 MHz and sweep time = 2 min.

2.5. Intracellular Ca^{2+} imaging

The experiments were performed in the external standard solution (in mM: 150 NaCl, 5 KCl, 2 $CaCl_2$, 1 $MgCl_2$, 10 glucose and 10 HEPES, pH 7.4 with Tris-OH) at room temperature as we reported previously (Kato et al., 2008; Mizoguchi et al., 2003, 2009). Intracellular Ca^{2+} concentration ($[Ca^{2+}]i$) in response to PMA application was monitored using fura-2 AM (acetoxymethyl ester) (Grynkiewicz et al., 1985) in rat primary microglial cells. The cells plated on glass-base dish were loaded with 5 μM fura-2 AM (Dojindo, Kumamoto, Japan) for 20 min and washed three times with HEPES buffer before the measurement. During the measurement, while using an inverted microscope (20×; Olympus IX70-22FL, Olympus Co. Tokyo, Japan), external HEPES buffer was constantly perfused (10 mL/min). For fura-2 excitation, the cells were illuminated with two alternating wavelengths, 340 and 380 nm using a computerized system. The emitted light was collected at 510 nm using a cooled CCD camera (C4742-95ER, Hamamatsu Photonics, Hamamatsu, Japan) and images were stored every 5 s. These series of sequential data were analyzed using the AquaCosmos software package (Hamamatsu photonics, Hamamatsu, Japan). The $[Ca^{2+}]i$ was calculated from the ratio (R) of fluorescence recorded at 340 and 380 nm excitation wavelengths for each pixel within a cell boundary (AquaCosmos software). Calibrations (conversion of R340/380 values into calcium concentrations) were performed as described previously (Grynkiewicz et al., 1985). Basal $[Ca^{2+}]i$ was determined from the initial 10 images of each cell recording. A $[Ca^{2+}]i$ signal was defined as an increase in R 340/380 with clear time correlation to the application of PMA.

Increase of $[Ca^{2+}]i$ in response to PMA application was calculated as difference between basal $[Ca^{2+}]i$ and highest $[Ca^{2+}]i$ during the treatment of PMA. All data presented were obtained from at least five dishes and three different cell preparations.

2.6. Morphology and immunofluorescence

NADPH oxidase activation via cytosolic $p47^{phox}$ protein translocation was investigated as previously described (Qian et al., 2008). The 6-3 cells were seeded in non-coated 6-well plates at 5×10^3 cells/well. They were incubated in both the absence and presence of aripiprazole, diphenylene iodonium (DPI) or apocynin for 5 h respectively, and then treated with 400 ng/mL PMA for 30 min. After being rinsed twice in 0.1 M Hepes/KOH, cells were fixed with 4% paraformaldehyde for 10 min, and then rinsed with 0.1 M Hepes/KOH for 10 min. The morphological changes of the cells were examined under phase contrast microscopy (Nikon, Tokyo, Japan). Indirect immunofluorescence was performed using the following antibodies: goat anti-$p47^{phox}$ polyclonal antibody which recognized $p47^{phox}$, a cytosolic, regulatory subunit of NADPH oxidase (1:100 dilution; Abcam, Cambridge, MA, USA) and rabbit anti-Iba-1 polyclonal antibody (1:400; Wako Pure Chemical Industries Ltd, Osaka, Japan). Cells were incubated in primary antibodies diluted in PBS containing 5% normal horse serum at 4 °C overnight. After rinsing twice with PBS for 5 min, anti-goat rhodamine-conjugated secondary antibody (Southern Biotech, Birmingham, AL, USA) and anti-rabbit fluorescein isothiocyanate (FITC)-conjugated secondary antibody (Southern Biotech, Birmingham, AL, USA) were used for detection. Fluorescent images were captured with fluorescence microscope (OLYMPUS BX50; Olympus Co. Ltd, Tokyo, Japan).

2.7. Co-culture experiment with microglial and neuronal cell lines

The PC12 cells were plated on 24-well tissue culture plates at a density of 2×10^3 cells per 1 mL per well and were then incubated in the presence of 20 ng/mL nerve growth factor (NGF) at 37 °C for 7–10 days enough to develop neuritic formation. The 6-3 microglial cells were plated on Tissue Culture Inserts for 24-well plates (Greiner Bio-One GmbH, Frickenhausen, Germany) at a density of 1×10^5 cells per 200 μL per well and were then pre-incubated in the presence of DMSO (0.05%) or aripiprazole (10 μM) for 5 h and then each Tissue Culture Inserts was placed on the 24-well tissue culture plate with PC12 cells, respectively. After 2 h co-incubation with 400 ng/mL PMA, Tissue Culture Inserts were removed from the 24-well plates with PC12 cells. Neuritic beading formations of PC12 cells were observed and assessed under a phase-contrast microscope as previously reported (Park et al., 1996; Takeuchi et al., 2005). More than 100 neurons in duplicate wells were assessed blindly in three independent trials. The ratio of the numbers of neuritic beading (beads) per one neuronal cell was calculated.

2.8. Statistics

Data were expressed as the means ± SEM and analyzed by a one-way analysis of variance (ANOVA) followed by Tukey's post hoc test. The significance was established at a level of $p<0.05$. All the data of each group were confirmed to be normally distributed by the Shapiro–Wilk test ($p>0.05$).

3. Results

3.1. Effects of the antipsychotics on the $\cdot O_2^-$ production by PMA-stimulated microglia

First of all, we directly measured the generation of $\cdot O_2^-$ associated with PMA-stimulated murine 6-3 microglia by ESR spectroscopy with a spin trap DEPMPO. In the preparations of non-stimulated microglia (Fig. 1A), no signals were obtained. Microglial cells stimulated by 400 ng/mL PMA in the presence of DEPMPO showed prominent signals whose spectra consisted of a linear combination of a characteristic 12-line spectrum corresponding to $\cdot O_2^-$ spin adduct DEPMPO–OOH and an 8-line spectrum corresponding to OH spin adduct DEPMPO–OH (Fig. 1B). Computer simulation confirmed DEPMPO–OOH with hyper-fine splittings $a_N = 13.15$ G, $a^b_H = 10{:}59$ G, $a_p = 49.73$ G, $a^g_H = 0{:}72$ G and DEPMPO–OH with hyper-fine splittings $a_N = 12.43$ G, $a_H = 13.49$ G, $a_p = 50.39$ G. These values are consistent with those described previously (Sankarapandi et al., 1998). Previously, we had demonstrated that the spin adducts originated from $\cdot O_2^-$ radical, but not •OH− radical, which is derived from H_2O_2 (Hashioka et al., 2007b). In the present study, the effects of various types of antipsychotics on the generation of $\cdot O_2^-$ from PMA-stimulated microglia were evaluated. Pretreatment with aripiprazole, a partial D2R agonist, for 5 h considerably inhibited the signal intensity of the $\cdot O_2^-$ adduct (Fig. 1C), while other antipsychotics with D2R antagonism including haloperidol, olanzapine, clozapine and risperidone did not have any inhibitory effect on the signal intensity of the $\cdot O_2^-$ adduct (Fig. 1D–G). In order to confirm whether the inhibitory effect of aripiprazole was due to D2R agonism or not, the effect of quinpirole which is a D2R full agonist was evaluated. Quinpirole did not have any inhibitory effect on the signal intensity of the $\cdot O_2^-$ adduct (Fig. 1H). These results thus suggested that the inhibitory effects of aripiprazole on the generation of $\cdot O_2^-$ from PMA-stimulated microglia were independent of the effects of aripiprazole on D2R. In addition, we also prepared rat primary microglial cells for ESR to confirm the relevance of our results in the 6-3 cells. In the case of PMA-stimulated rat primary microglial cells, the $\cdot O_2^-$ like adduct was measured despite a very low signal intensity due to much smaller quantity of the rat primary microglial cells (1.6×10^4) than that of the 6-3 cells (1.6×10^6) (Fig. 2B). Aripiprazole considerably reduced the signal intensity of the above-mentioned $\cdot O_2^-$ like adduct (Fig. 2C). These results suggest that the inhibitory effects of aripiprazole on microglial activation were not limited to the 6-3 microglia. To confirm whether or not aripiprazole per se scavenges $\cdot O_2^-$, we measured the $\cdot O_2^-$ production in xanthine/xanthine oxidase system in both the presence and absence of aripiprazole by ESR monitoring with a spin trap DEPMPO. Fig. 3A shows typical ESR spectra consisting of DEPMPO–OOH and DEPMPO–OH in xanthine/xanthine oxidase system. The formation of these spin adducts via trapping $\cdot O_2^-$ was confirmed by our previous report (Hashioka et al., 2007b). The ESR spectra in the presence of aripiprazole (Fig. 3B) proved to be essentially the same as those shown in Fig. 3A, thus indicating that aripiprazole does not have scavenging effect on $\cdot O_2^-$. Similarly, other antipsychotics did not show any scavenging effect of $\cdot O_2^-$ (data not shown).

Since assays of free-radical production in cells are notoriously capricious (Abramov et al., 2005), in order to reinforce the ESR evidence above, we also quantified $\cdot O_2^-$ generation by the NBT assay. We observed that application of PMA significantly induced $\cdot O_2^-$ release from both the rat primary microglial cells (Fig. 4A) and the 6-3 microglial cells (Fig. 4B). Pretreatment with aripiprazole for 5 h significantly inhibited the $\cdot O_2^-$ release from PMA-stimulated microglial cells in comparison to the positive control, however, pretreatment of haloperidol and quinpirole did not have any inhibitory effects at all (Fig. 4B). In addition, we confirmed that 2 h-pretreatment of aripiprazole also inhibited the $\cdot O_2^-$ release dose-dependently (Fig. 4C). These results thus confirmed the relevance of the ESR results.

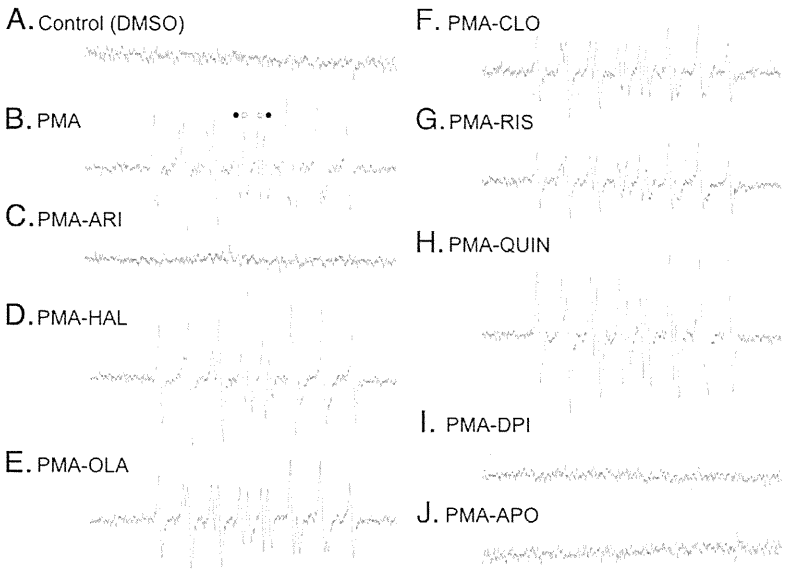

Fig. 1. Detection of $\cdot O_2^-$ generation by PMA-stimulated 6-3 microglial cells using ESR spin trap technique with DEPMPO. Murine 6-3 microglial cells (4×10^6/mL) were prepared and incubated with PMA (400 ng/mL) for 30 min at 37 °C with and without pretreatment of antipsychotics for 5 h. The ESR spectra were then recorded in the presence of 25 mM DEPMPO at room temperature. (A) ESR spectra of DEPMPO adducts obtained from non-stimulated microglia. (B) ESR spectra of DEPMPO adducts obtained from PMA-stimulated microglia. Open and closed circles represent measured signal peaks of DEPMPO–OH and DEPMPO–OOH adducts, respectively. (C) ESR spectra of DEPMPO adducts obtained from microglia stimulated by PMA (400 ng/mL) after a 5 h pretreatment with aripiprazole (10 μM). (D) The same as (C) but with haloperidol (10 μM). (E) The same as (C) but with olanzapine (10 μM). (F) The same as (C) but with clozapine (10 μM). (G) The same as (C) but with risperidone (10 μM). (H) The same as (C) but with quinpirole (10 μM). (I) The same as (C) but with DPI (10 μM). (J) The same as (C) but with apocynin (1 μM).

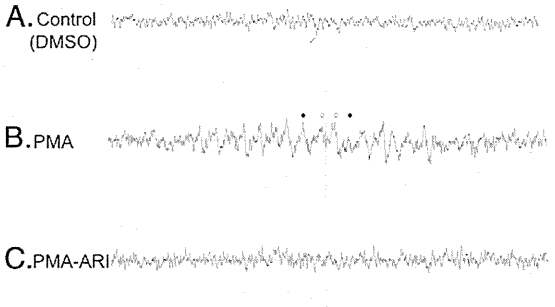

Fig. 2. Detection of $\cdot O_2^-$ generation by PMA-activated rat primary microglial cells using ESR spin trap technique with DEPMPO. Rat primary microglial cells (4×10^4/mL) were prepared and incubated with PMA (400 ng/mL) for 30 min at 37 °C with and without pretreatment of aripiprazole for 5 h. The ESR spectra were then recorded in the presence of 25 mM DEPMPO at room temperature. (A) ESR spectra of DEPMPO adducts obtained from non-stimulated microglia. (B) ESR spectra of DEPMPO adducts obtained from PMA-stimulated microglia. Open and closed circles represent measured signal peaks of DEPMPO–OH and DEPMPO–OOH adducts, respectively. (C) ESR spectra of DEPMPO adducts obtained from microglia stimulated by PMA (400 ng/mL) after a 5 h pretreatment with aripiprazole (10 μM).

3.2. Aripiprazole inhibits PMA-induced translocation of NADPH oxidase cytosolic subunit of PHOX p47^{phox} to the plasma/phagosomal membranes

In the ESR experiments, not only aripiprazole but also NADPH oxidase inhibitors (diphenylene iodonium (DPI) and apocynin) proved to have a considerable inhibitory effect on PMA-induced $\cdot O_2^-$ generation from the murine microglial cells (Fig. 1I and J). Therefore, our results suggest that the $\cdot O_2^-$ generation in the microglial cells depends on NADPH oxidase pathway as previously reported (Sankarapandi et al., 1998). Inhibitory process of NADPH oxidase is reported to be different between DPI and apocynin: apocynin inhibits the translocation of subunits such as p47 and p67 in cytosol, while DPI acts by abstracting an electron from an electron transporter and forming a radical, which then inhibits the respective electron transporter through a covalent binding step in membrane (Bedard and Krause, 2007).

In the DMSO treatment group, the 6-3 cells showed typical resting morphology with small cell bodies (Fig. 5A). On the other hand, PMA-

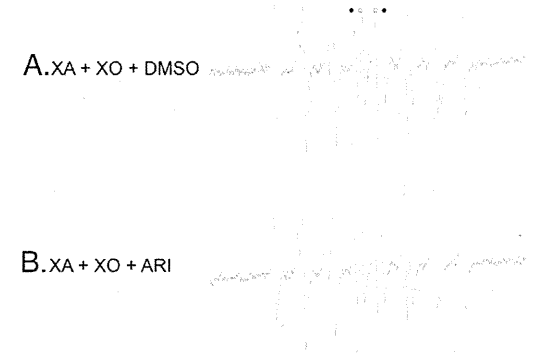

Fig. 3. Detection of $\cdot O_2^-$ generation in xanthine/xanthine oxidase system using ESR spin trap technique with DEPMPO. The system contained 0.4 mM xanthine, 2 mM DTPA, and 20 mM DEPMPO in PB in the presence and absence of 10 μM aripiprazole. Xanthine oxidase (0.1 U/mL) was added last to the mixture to start the reaction. (A) ESR spectra of DEPMPO adducts obtained in the xanthine/xanthine oxidase system in the presence of the control DMSO (final concentration: 0.05%). Open and closed circles represent measured signal peaks of DEPMPO–OH and DEPMPO–OOH adducts, respectively. (B) The same as (A), but also in the presence of aripiprazole (10 μM).

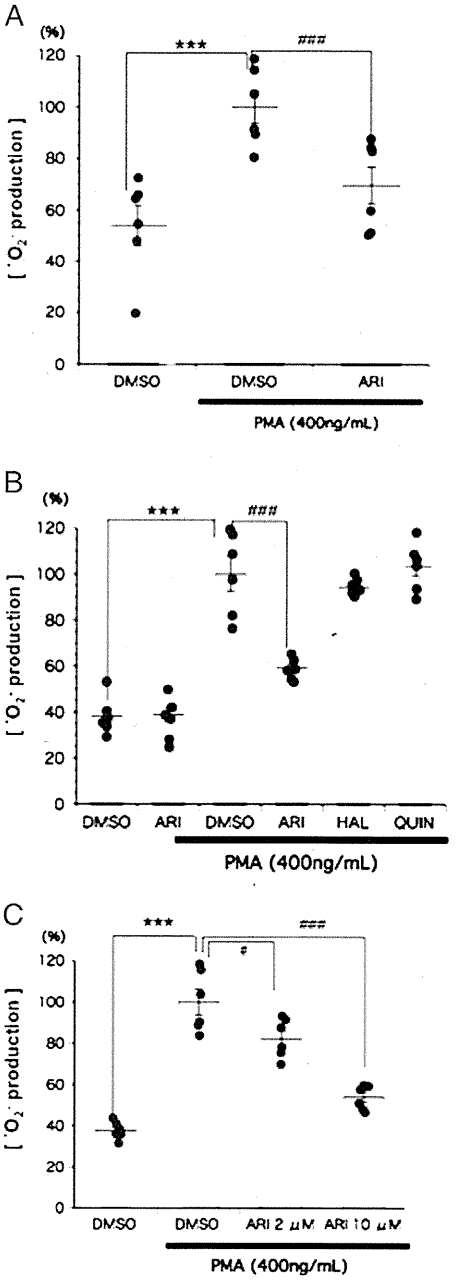

Fig. 4. Quantification of $\cdot O_2^-$ production in microglial cells by Nitro blue tetrazolium (NBT) assay. (A) The rat primary microglial cells were pre-treated with DMSO (0.05%) and aripiprazole (10 μM) for 5 h, then the cells were treated with PMA (400 ng/mL) for 30 min. The $\cdot O_2^-$ production was determined using the NBT assay. The results were expressed as percentage values taking the PMA + DMSO treatment group as 100%. (B) The mouse 6-3 microglial cells were pre-treated with DMSO (0.05%), aripiprazole (10 μM), haloperidol (10 μM) and quinpirole (10 μM) for 5 h, then the cells were treated with PMA (400 ng/mL) for 30 min. The $\cdot O_2^-$ production was determined using the NBT assay. The results were expressed as percentage values taking the PMA + DMSO treatment group as 100%. All data are represented as the means (SEM) of three independent experiments (n = 6–9). ***P<0.001 in comparison to the control DMSO treatment group. ###P<0.001 in comparison to the PMA + DMSO treatment group. (C) The mouse 6-3 microglial cells were pre-treated with DMSO (0.05%) and aripiprazole (10 μM) for 2 h, then the cells were treated with PMA (400 ng/mL) for 30 min. The $\cdot O_2^-$ production was determined using the NBT assay. The results were expressed as percentage values taking the PMA + DMSO treatment group as 100%. All data are represented as the means (SEM) of three independent experiments (n = 6–9). ***P<0.001 in comparison to the control DMSO treatment group. #P<0.05/###P<0.001 in comparison to the PMA + DMSO treatment group.

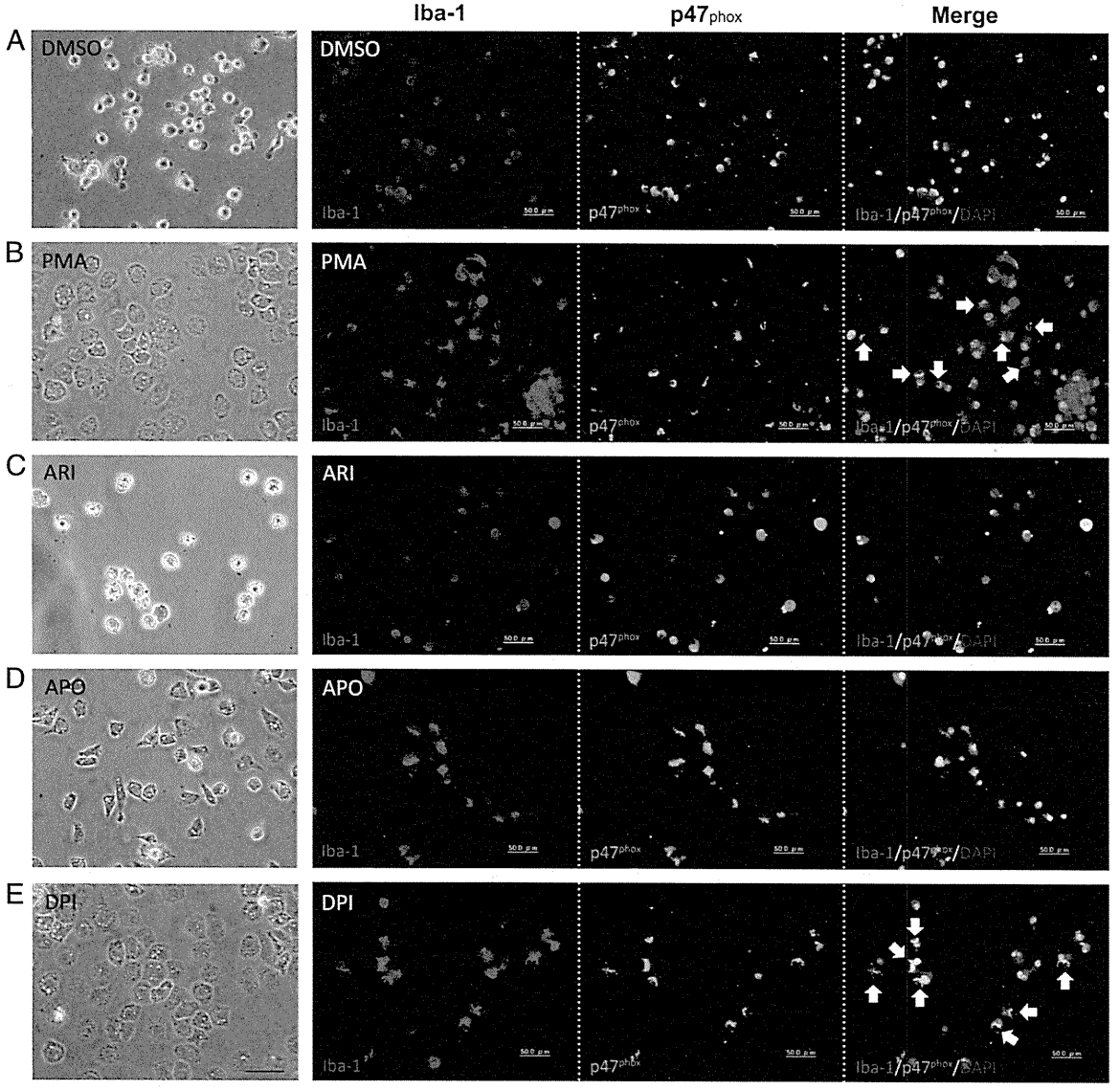

Fig. 5. Microglial cell morphology and cytosolic p47^{phox} protein translocation. Cell morphology of the murine 6-3 microglia is shown in the leftmost line, and the existence of cytosolic Iba-1 (red), p47^{phox} (green) and nuclear (DAPI; blue) is shown in the second-leftmost line, second-rightmost line and rightmost line, respectively. In the absence of PMA, cells showed resting shapes and p47^{phox} was localized in the cytosol (A). Both PMA-treatment cells and DPI-pretreatment cells showed ameboid shapes and p47^{phox} was translocated to the plasma/phagosomal membranes, especially phagosomal membranes inside the cytosol with a ring structure (arrows) (B and E). Both aripiprazole- and apocynin-pretreatment cells showed spindle shapes and p47^{phox} was localized in the cytosol without ring structures (C and D). Scale bar indicates 50 μm.

treated 6-3 cells underwent ameboid shapes with cytoplasmic vacuoles (Fig. 5B). DPI-pretreated cells were also changed to ameboid shape morphology after PMA-stimulation (Fig. 5D). Aripiprazole- or apocynin-pretreated cells followed by PMA-stimulation were exhibited in various types of morphology, including roundish and multipolar spindle shapes (Fig. 5C and E).

Activation of NADPH oxidase has been reported to require phosphorylation and subsequent translocation of the cytosolic component p47^{phox}, together with other NADPH oxidase cytoplasmic subunits to the plasma membrane and/or the phagosomal membranes in the cytoplasm (Bedard and Krause, 2007; Liva et al., 1999). As aripiprazole considerably inhibits $\bullet O_2^-$ production induced by PMA, we sought to determine whether aripiprazole inhibits NADPH oxidase activation by preventing the translocation of p47^{phox} from the cytosol to the membranes after PMA stimulation. Immunostaining for the p47^{phox} demonstrated that cytosolic p47^{phox} was formed ring-like structure after PMA treatment in the cytoplasm (Fig. 5B), suggesting that phosphorylated p47^{phox} was mainly translocated to the phagosomal membranes. Aripiprazole- or apocynin-preincubated cells were prevented this formation (Fig. 5C and D). In DPI-pretreated cells, p47^{phox} was also formed ring-like structure as well as PMA-treated cells (Fig. 5E). In cells treated with DMSO alone in the absence of PMA stimulation, p47^{phox} remained localized primarily in the cytosol (Fig. 5A).

Therefore, one mechanism by which aripiprazole inhibits $\bullet O_2^-$ production in microglial cells seems to be through the inhibition of p47^{phox} translocation to the membranes after PMA stimulation, which is similar to the inhibitory process of apocynin.

3.3. Aripiprazole attenuates the mobilization of intracellular Ca^{2+} induced by PMA in microglia

Next, we investigated the effect of aripiprazole on the mobilization of intracellular Ca^{2+} induced by PMA in rat primary microglia. PMA are known to induce $\cdot O_2^-$ from microglia with the elevation of intracellular Ca^{2+} (Colton et al., 1992; Yoo et al., 1996). In the present study, we observed that PMA (400 ng/mL) acutely induced a transient increase in $[Ca^{2+}]i$ in the rat primary microglia (n = 50 cells; Fig. 6A and C), as previously reported in human microglia (Yoo et al., 1996). Pretreatment of 5 μM aripiprazole for 5 h attenuated the PMA-induced increase in $[Ca^{2+}]i$ (n = 18 cells; Fig. 6B and C). Pretreatment of 1 μM apocynin also attenuated the PMA-induced increase in $[Ca^{2+}]i$ (n = 5 cells; Fig. 6C), while pretreatment of 10 μM DPI did not affect the PMA-induced increase in $[Ca^{2+}]i$ in the rat microglial cells (n = 29 cells; Fig. 6C).

3.4. Aripiprazole attenuates the production of neuritic beading induced by activated microglia

Finally, neuronal damage induced by microglial activation was investigated with the co-culture experiment. Presence of neuritic bead is one of the earliest outcomes of neuronal damage (Park et al., 1996; Takeuchi et al., 2005). PMA-treatment with 6-3 microglial cells for 2 h obviously induced neuritic beading of PC12 cells (Fig. 7A, B and D). Pretreatment of aripiprazole for 5 h significantly reduced the formation of neuritic beading (Fig. 7C and D). Our results indicate that aripiprazole protected from formation of neuritic beading induced by PMA-stimulated microglial activation.

4. Discussion

This is the first report to demonstrate that among typical and atypical antipsychotics, only aripiprazole inhibited the generation of $\cdot O_2^-$ from PMA-stimulated microglia. Aripiprazole proved to inhibit the generation of $\cdot O_2^-$ through the cascade of PKC activation, intracellular Ca^{2+} regulation and NADPH oxidase activation in microglial cells. In addition, aripiprazole indicated to have neuroprotective effects via inhibiting microglial activation by the co-culture experiment.

The typical dose range of aripiprazole is 10–30 mg/day and the typical serum concentration or plasma range of aripiprazole is 0–1000 ng/mL (0–2 μM) (Alexopoulos et al., 2004; Chew et al., 2006; Grunder et al., 2008). Antipsychotics are known to accumulate in brain tissue to levels that are 25–30 fold higher than serum levels (Baumann et al., 2004). Therefore, in spite of no evidence that the effect of a drug in cell culture could be compared to the effect of the same drug at a brain tissue level even in the same range of concentration, the concentrations of aripiprazole used in the present study might thus not be substantially different from the brain tissue levels for aripiprazole. The same concentrations were applied to other antipsychotics (haloperidol, olanzapine, clozapine and risperidone) according to previously published in vitro studies using microglial cells (Hou et al., 2006; Kato et al., 2007, 2008).

Aripiprazole is a high-affinity D2R partial agonist, while other antipsychotics investigated in the present study are all D2R antagonists (Burris et al., 2002; Shapiro et al., 2003). These differences may be relevant to the results shown in the present study. Farber et al. provided the first evidence of the existence of functional dopamine receptors on microglia. In their study, quinpirole inhibited the release of NO from LPS-induced microglia dose-dependently (Farber et al., 2005). On the other hand, in our previous study, not quinpirole but aripiprazole showed inhibitory effects on the generation of NO and TNF-α from interferon-γ-stimulated microglia (Kato et al., 2008). Moreover, in the present study, quinpirole did not have any inhibitory effects on the generation of $\cdot O_2^-$ from PMA-stimulated microglia. These results seem to suggest that the dopamine D_2 receptors may not be involved in the generation of $\cdot O_2^-$ from PMA-stimulated microglia and in the inhibition of $\cdot O_2^-$ production by aripiprazole shown in the present study. Aripiprazole has affinities of other receptors such as

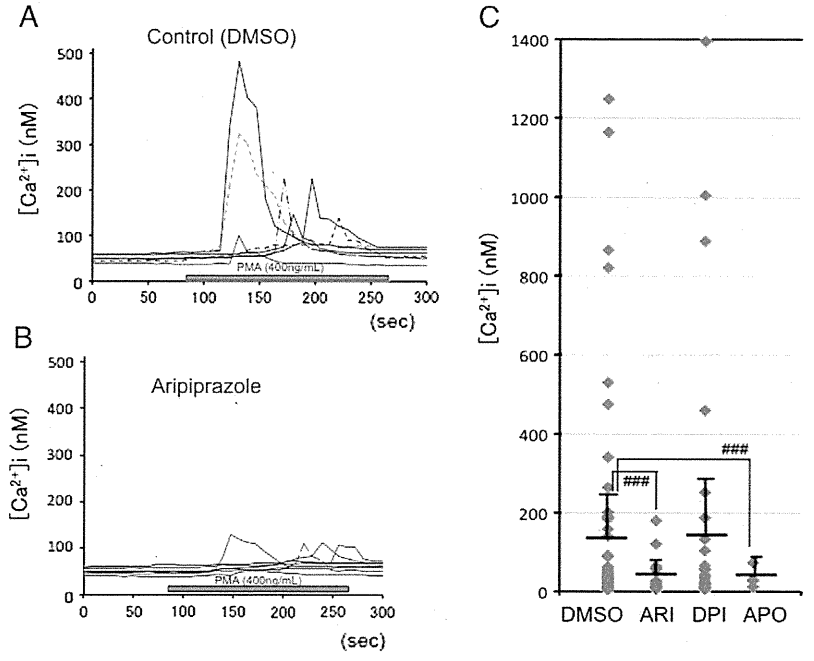

Fig. 6. Aripiprazole attenuates the mobilization of intracellular Ca^{2+} induced by PMA in rat microglia. (A and B) Seven representative traces showing a brief application (3 min) of 400 ng/mL PMA induced a transient increase in $[Ca^{2+}]i$ in rat microglia pretreated with DMSO (0.025%; in A) and with aripiprazole (5 μM; in B). (C) Bar graph summarizing the effect of different manipulations on the peak amplitude of PMA-induced increase in $[Ca^{2+}]i$ in rat microglia. Increase of $[Ca^{2+}]i$ in response to PMA application with DMSO, aripiprazole, DPI and apocynin was calculated as a difference between basal $[Ca^{2+}]i$ and highest $[Ca^{2+}]i$ during the treatment of PMA, respectively. All data presented were obtained from at least five dishes and three different cell preparations. Data are expressed as the mean ± SEM. ###P<0.001 in comparison to the PMA + DMSO treatment group.

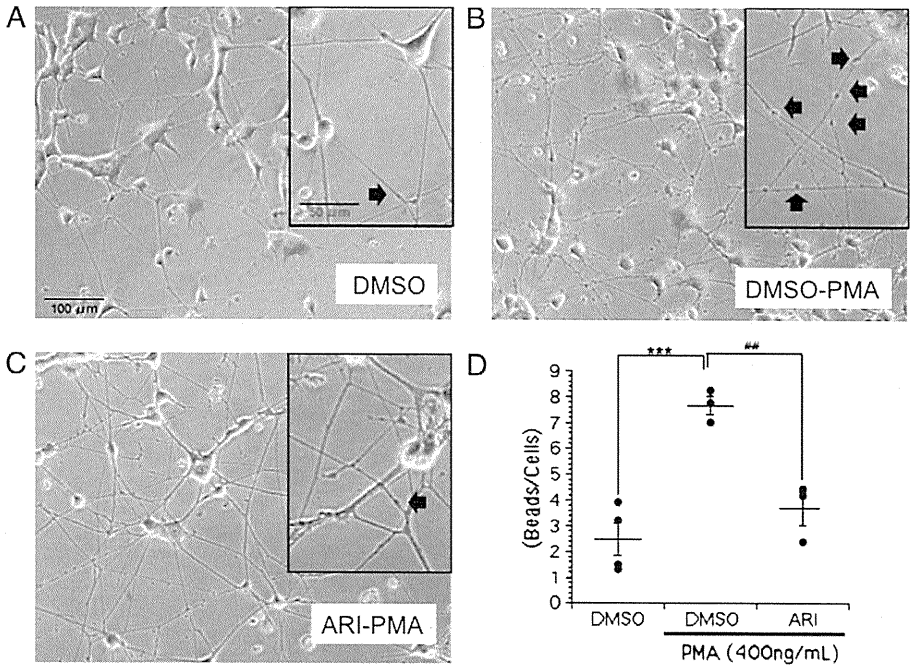

Fig. 7. Neuritic beading induced by PMA-stimulated microglia. Neuritic formation of the PC12 cells, which was taken under a phase-contrast microscope, is shown in the main photo and enhanced photo is shown in the upper right-hand corner (enhanced) (A–C). (A) Pretreatment with DMSO (0.05%), following co-culture with the 6-3 microglial cells without PMA treatment for 2 h. (B) Pretreatment with DMSO (0.05%), following co-culture with the 6-3 microglial cells with 400 ng/mL PMA treatment for 2 h. (C) Pretreatment with aripiprazole (10 μM), following co-culture with the 6-3 microglial cells with 400 ng/mL PMA treatment for 2 h. (D) Quantification of neuritic beading. The number of neuritic beading (beads) under more than 100 neuronal cell bodies was assessed blindly in three independent trials. All data are expressed the means (SEM) of the number of neuritic beading (beads) per one neuronal cell (each: 3–4 trials). ***P<0.001 in comparison to the control DMSO treatment group. ##P<0.01 in comparison to the DMSO + PMA treatment group.

serotonin (Shapiro et al., 2003). Our recent study has proved that not only antipsychotics but also antidepressants have inhibitory effects of microglial activation (Horikawa et al., 2010), which indicate that other pharmacological mechanism beyond D2R may exist in our findings. Further investigation is required in order to clarify the underlying mechanism.

We showed the first evidence that aripiprazole attenuates the mobilization of intracellular Ca^{2+} induced by PMA in rat microglia. PMA is known to induce $\cdot O_2^-$ from microglia with the elevation of intracellular Ca^{2+} (Colton et al., 1992; Yoo et al., 1996). Intracellular Ca^{2+} is one of the endogenous activators of PKC. Regarding mammalian astrocytes, PMA proved to activate the NADPH oxidase through the activation of PKC, while the elevation of intracellular Ca^{2+} induced by PMA itself activates the NADPH oxidase independently of PKC (Abramov et al., 2005). We showed that aripiprazole inhibits NADPH oxidase activation by preventing the translocation of $p47^{phox}$ from the cytosol to the membrane after PMA stimulation. Our results suggest that the $\cdot O_2^-$ generation in the microglial cells depends on NADPH oxidase pathway, inhibitory effects of which are similar not to DPI but to apocynin. Summing up these results, aripiprazole indicates to inhibit the $\cdot O_2^-$ generation through the NADPH oxidase by suppressing the elevation of intracellular Ca^{2+} in PMA-treated microglia.

Antioxidants have recently been regarded to have protective effects in neurodegeneration, and microglial activation via NADPH oxidase has a key role in this process (Wang et al., 2006). NADPH-derived ROS such as $\cdot O_2^-$ and •OH radicals have been reported not only to cause microglial proliferation but also to amplify the proinflammatory gene expressions, both of which are associated with neurotoxicity induced by activated microglia (Pawate et al., 2004; Qin et al., 2004). In our previous study, risperidone and other atypical antipsychotics with D2R antagonism inhibited the production of proinflammatory cytokines (Bian et al., 2008; Kato et al., 2007), however these antipsychotics have no inhibitory effect of releasing $\cdot O_2^-$ radicals from activated microglia in the present study. On the other hand, aripiprazole proved to have dual inhibitory effects of releasing pro-inflammatory cytokines (Kato et al., 2008) and $\cdot O_2^-$ radicals from activated microglia in the present study. Therefore, we presume aripiprazole to be the strongest antioxidative/anti-inflammatory agent among antipsychotics.

We previously demonstrated that aripiprazole inhibits microglial activation induced by IFN-γ and suggested that this inhibitory effect is related to the inhibition of the cell signaling pathways including PKC, p38MAPK, and ERK (Kato et al., 2008). PMA is a PKC activator and PKC pathway is located in the upstream of both p38MAPK and ERK pathways in the process of PMA-induced microglial activation as shown in Nikodemova et al. (2006). Therefore, the inhibitory effects of aripiprazole on neuritic beading which was shown in the present co-culture study is probably due to the inhibitory effects of aripiprazole on the generation of both $\cdot O_2^-$ and pro-inflammatory cytokines from PMA-stimulated microglia.

Structural brain abnormalities such as progressive gray matter loss have been extensively and consistently described in schizophrenic patients (Davis et al., 2003; Kumra et al., 2005). This evidence is the primarily propounded mechanism explaining the neurodegenerative course of schizophrenia (Salisbury et al., 2007). Multiple lines of evidence combine to implicate the increased susceptibility to apoptotic death in the pathophysiology of schizophrenia (Glantz et al., 2006). The activation of apoptotic process can lead to a rapid neuronal death (Glantz et al., 2006; Jarskog et al., 2005). Microglial NADPH oxidase pathway has recently been reported to play a key role in the process of neuronal deaths (Qin et al., 2006). Furthermore, our results of co-culture experiment suggest that activation of microglial NADPH oxidase pathway induces neuritic beading formation, which is one of the initial steps of neuronal damage (Park et al., 1996; Takeuchi et al., 2005). In addition, aripiprazole attenuated the neuritic beading formation, which indicates that aripiprazole may be a neuroprotective agent via inhibiting microglial activation. One recent animal study

indicates that aripiprazole prevents apoptosis in the brain of methamphetamine-treatment rodents. (Abekawa et al., 2011), which supports the significance of our results.

Recent neuroimaging studies have shown significant volume reductions in white matter with abnormal brain connectivity in schizophrenia (Schlosser et al., 2007). The reduced density and compromised morphology of the oligodendrocytes as well as signs of deviant myelination have been evident in schizophrenia (Uranova et al., 2007). Microglial activation in the CNS has been implicated in the pathogenesis of white matter disorders, and microglial cytotoxicity of oligodendrocyte has been reported to mediate through the free radical-related molecules such as NO, $\bullet O_2^-$ and their compound, peroxynitrite ($ONOO^-$) generated by activated microglia (Li et al., 2005; Merrill et al., 1993). On the other hand, one recent imaging report suggests that risperidone, which have anti-inflammatory effects on microglial activation in vitro (Kato et al., 2007), may be specifically impacting later-myelinating intracortical circuitry in patients with schizophrenia (Bartzokis et al., 2009).

Summing up the aforementioned evidence and our results, aripiprazole may thus have therapeutic effects on patients with schizophrenia by reducing the microglial inflammatory/oxidative reactions, which puts forward a novel therapeutic hypothesis beyond dopamine/neuron doctrine in the field of schizophrenia research. Besides schizophrenia, aripiprazole has proved to have therapeutic effects in depression, anxiety and other psychiatric disorders (Mohamed et al., 2009; Weber et al., 2008). In a recent animal study, aripiprazole has proved to have protective effects on the depression-induced oxidative stress in rat brain (Eren et al., 2007). This evidence has accorded with our present result that except for aripiprazole no other antipsychotics have an antioxidative effect via inhibiting superoxide generation from activated microglia. Thus, such wider range of aripiprazole pharmacological effects on various psychiatric diseases may be explained by the present result that aripiprazole inhibits the microglia-induced oxidative stress.

The brain is considered particularly vulnerable to oxidative damage. This intrinsic oxidative vulnerability of the brain suggests that oxidative damage may be a plausible pathogenic candidate of schizophrenia, depression and other psychiatric disorders (Ng et al., 2008). Therefore, our results may imply that aripiprazole acts, at least partially, by a different mechanism of action than other antipsychotics, which may be reflected in its deviating clinical profile. Regarding further studies, the molecular mechanism of the inhibitory effect of aripiprazole on the generation of $\bullet O_2^-$ radicals from PMA-stimulated microglia should be clarified in more detail, and in vivo studies should also be performed in order to confirm the present results.

Role of funding source

This work was financially supported by Grant-in-Aid for Research Fellow of the Japan Society for the Promotion of Science (JSPS) [to TAK] and for researchers from JSPS [to TAK, AM, YM and SK], and by Grant-in-Aid for Mitsubishi Pharma Research Foundation [to TAK and AM].

Contributors

All authors contributed substantially to the scientific process leading up to the writing of the present paper. TAK, the first author, and AM, the principal investigator of the present research made the conception and design of the project and wrote the protocol. The performance of experiments and the data analysis/interpretation were done by TAK, AM, KY, YM, HH, YS, SH, YHH, NS, EH and YM. TAK wrote the first draft of the manuscript. Critical revisions of the manuscript were made by TI, HU and SK. All authors contributed to and have approved the final manuscript.

Conflict of interest

All authors declare that they have no financial conflict of interest.

Acknowledgments

The authors thank Prof. Makoto Sawada of Nagoya University for providing the microglial cell line, 6-3. The authors also thank Dr. Tomoaki Inoue and Ms. Mayumi Tanaka for his/her experimental assistance.

References

Abekawa, T., Ito, K., Nakagawa, S., Nakato, Y., Koyama, T., 2011. Effects of aripiprazole and haloperidol on progression to schizophrenia-like behavioural abnormalities and apoptosis in rodents. Schizophr. Res. 125, 77–87.

Abramov, A.Y., Jacobson, J., Wientjes, F., Hothersall, J., Canevari, L., Duchen, M.R., 2005. Expression and modulation of an NADPH oxidase in mammalian astrocytes. J. Neurosci. 25, 9176–9184.

Akhondzadeh, S., Tabatabaee, M., Amini, H., Ahmadi Abhari, S.A., Abbasi, S.H., Behnam, B., 2007. Celecoxib as adjunctive therapy in schizophrenia: a double-blind, randomized and placebo-controlled trial. Schizophr. Res. 90, 179–185.

Alexopoulos, G.S., Streim, J., Carpenter, D., Docherty, J.P., 2004. Using antipsychotic agents in older patients. J. Clin. Psychiatry 65 (Suppl 2), 5–104.

Bartzokis, G., Lu, P.H., Stewart, S.B., Oluwadara, B., Lucas, A.J., Pantages, J., Pratt, E., Sherin, J.E., Altshuler, L.L., Mintz, J., Gitlin, M.J., Subotnik, K.L., Nuechterlein, K.H., 2009. In vivo evidence of differential impact of typical and atypical antipsychotics on intracortical myelin in adults with schizophrenia. Schizophr. Res. 113, 322–331.

Baumann, P., Hiemke, C., Ulrich, S., Eckermann, G., Gaertner, I., Gerlach, M., Kuss, H.J., Laux, G., Muller-Oerlinghausen, B., Rao, M.L., Riederer, P., Zernig, G., Arbeitsgemeinschaft fur neuropsychopharmakologie und p, 2004. The AGNP-TDM expert group consensus guidelines: therapeutic drug monitoring in psychiatry. Pharmacopsychiatry 37, 243–265.

Bedard, K., Krause, K.H., 2007. The NOX family of ROS-generating NADPH oxidases: physiology and pathophysiology. Physiol. Rev. 87, 245–313.

Behrens, M.M., Ali, S.S., Dao, D.N., Lucero, J., Shekhtman, G., Quick, K.L., Dugan, L.L., 2007. Ketamine-induced loss of phenotype of fast-spiking interneurons is mediated by NADPH-oxidase. Science 318, 1645–1647.

Berk, M., Copolov, D., Dean, O., Lu, K., Jeavons, S., Schapkaitz, I., Anderson-Hunt, M., Judd, F., Katz, F., Katz, P., Ording-Jespersen, S., Little, J., Conus, P., Cuenod, M., Do, K.Q., Bush, A.I., 2008. N-acetyl cysteine as a glutathione precursor for schizophrenia—a double-blind, randomized, placebo-controlled trial. Biol. Psychiatry 64, 361–368.

Bian, Q., Kato, T., Monji, A., Hashioka, S., Mizoguchi, Y., Horikawa, H., Kanba, S., 2008. The effect of atypical antipsychotics, perospirone, ziprasidone and quetiapine on microglial activation induced by interferon-gamma. Prog. Neuropsychopharmacol. Biol. Psychiatry 32, 42–48.

Block, M.L., Hong, J.S., 2005. Microglia and inflammation-mediated neurodegeneration: multiple triggers with a common mechanism. Prog. Neurobiol. 76, 77–98.

Block, M.L., Zecca, L., Hong, J.S., 2007. Microglia-mediated neurotoxicity: uncovering the molecular mechanisms. Nat. Rev. Neurosci. 8, 57–69.

Burris, K.D., Molski, T.F., Xu, C., Ryan, E., Tottori, K., Kikuchi, T., Yocca, F.D., Molinoff, P.B., 2002. Aripiprazole, a novel antipsychotic, is a high-affinity partial agonist at human dopamine D2 receptors. J. Pharmacol. Exp. Ther. 302, 381–389.

Chen, G., Henter, I.D., Manji, H.K., 2009. A role for PKC in mediating stress-induced prefrontal cortical structural plasticity and cognitive function. Proc. Natl Acad. Sci. U.S.A. 106, 17613–17614.

Chew, M.L., Mulsant, B.H., Pollock, B.G., Lehman, M.E., Greenspan, A., Kirshner, M.A., Bies, R.R., Kapur, S., Gharabawi, G., 2006. A model of anticholinergic activity of atypical antipsychotic medications. Schizophr. Res. 88, 63–72.

Choi, H.S., Kim, J.W., Cha, Y.N., Kim, C., 2006. A quantitative nitroblue tetrazolium assay for determining intracellular superoxide anion production in phagocytic cells. J. Immunoassay Immunochem. 27, 31–44.

Colton, C.A., Yao, J., Keri, J.E., Gilbert, D., 1992. Regulation of microglial function by interferons. J. Neuroimmunol. 40, 89–98.

Dalman, C., Allebeck, P., Gunnell, D., Harrison, G., Kristensson, K., Lewis, G., Lofving, S., Rasmussen, F., Wicks, S., Karlsson, H., 2008. Infections in the CNS during childhood and the risk of subsequent psychotic illness: a cohort study of more than one million Swedish subjects. Am. J. Psychiatry 165, 59–65.

Davis, K.L., Stewart, D.G., Friedman, J.I., Buchsbaum, M., Harvey, P.D., Hof, P.R., Buxbaum, J., Haroutunian, V., 2003. White matter changes in schizophrenia: evidence for myelin-related dysfunction. Arch. Gen. Psychiatry 60, 443–456.

Do, K.Q., Cabungcal, J.H., Frank, A., Steullet, P., Cuenod, M., 2009. Redox dysregulation, neurodevelopment, and schizophrenia. Curr. Opin. Neurobiol. 19, 220–230.

Doorduin, J., de Vries, E., Willemsen, A., de Groot, J., Dierckx, R., Klein, H., 2009. Neuroinflammation in schizophrenia-related psychosis: a PET study. J. Nucl. Med. 50, 1801–1807.

Eren, I., Naziroglu, M., Demirdas, A., 2007. Protective effects of lamotrigine, aripiprazole and escitalopram on depression-induced oxidative stress in rat brain. Neurochem. Res. 32, 1188–1195.

Farber, K., Pannasch, U., Kettenmann, H., 2005. Dopamine and noradrenaline control distinct functions in rodent microglial cells. Mol. Cell. Neurosci. 29, 128–138.

Glantz, L.A., Gilmore, J.H., Lieberman, J.A., Jarskog, L.F., 2006. Apoptotic mechanisms and the synaptic pathology of schizophrenia. Schizophr. Res. 81, 47–63.

Grunder, G., Fellows, C., Janouschek, H., Veselinovic, T., Boy, C., Brocheler, A., Kirschbaum, K.M., Hellmann, S., Spreckelmeyer, K.M., Hiemke, C., Rosch, F., Schaefer, W.M., Vernaleken, I., 2008. Brain and plasma pharmacokinetics of aripiprazole in patients with schizophrenia: an [18F]fallypride PET study. Am. J. Psychiatry 165, 988–995.

Grynkiewicz, G., Poenie, M., Tsien, R.Y., 1985. A new generation of Ca^{2+} indicators with greatly improved fluorescence properties. J. Biol. Chem. 260, 3440–3450.

Hains, A.B., Vu, M.A., Maciejewski, P.K., van Dyck, C.H., Gottron, M., Arnsten, A.F., 2009. Inhibition of protein kinase C signaling protects prefrontal cortex dendritic spines and cognition from the effects of chronic stress. Proc. Natl Acad. Sci. U.S.A. 106, 17957–17962.

Hanisch, U.K., Kettenmann, H., 2007. Microglia: active sensor and versatile effector cells in the normal and pathologic brain. Nat. Neurosci. 10, 1387–1394.

Hashioka, S., Han, Y.H., Fujii, S., Kato, T., Monji, A., Utsumi, H., Sawada, M., Nakanishi, H., Kanba, S., 2007a. Phosphatidylserine and phosphatidylcholine-containing liposomes inhibit amyloid beta and interferon-gamma-induced microglial activation. Free Radic. Biol. Med. 42, 945–954.
Hashioka, S., Han, Y.H., Fujii, S., Kato, T., Monji, A., Utsumi, H., Sawada, M., Nakanishi, H., Kanba, S., 2007b. Phospholipids modulate superoxide and nitric oxide production by lipopolysaccharide and phorbol 12-myristate-13-acetate-activated microglia. Neurochem. Int. 50, 499–506.
Horikawa, H., Kato, T.A., Mizoguchi, Y., Monji, A., Seki, Y., Ohkuri, T., Gotoh, L., Yonaha, M., Ueda, T., Hashioka, S., Kanba, S., 2010. Inhibitory effects of SSRIs on IFN-gamma induced microglial activation through the regulation of intracellular calcium. Prog. Neuropsychopharmacol. Biol. Psychiatry 34, 1306–1316.
Hou, Y., Wu, C.F., Yang, J.Y., He, X., Bi, X.L., Yu, L., Guo, T., 2006. Effects of clozapine, olanzapine and haloperidol on nitric oxide production by lipopolysaccharide-activated N9 cells. Prog. Neuropsychopharmacol. Biol. Psychiatry 30 (8), 1523–1528.
Jarskog, L.F., Glantz, L.A., Gilmore, J.H., Lieberman, J.A., 2005. Apoptotic mechanisms in the pathophysiology of schizophrenia. Prog. Neuropsychopharmacol. Biol. Psychiatry 29, 846–858.
Jia, P., Wang, L., Meltzer, H.Y., Zhao, Z., 2010. Common variants conferring risk of schizophrenia: a pathway analysis of GWAS data. Schizophr. Res. 122, 38–42.
Kanzawa, T., Sawada, M., Kato, K., Yamamoto, K., Mori, H., Tanaka, R., 2000. Differentiated regulation of allo-antigen presentation by different types of murine microglial cell lines. J. Neurosci. Res. 62, 383–388.
Kapur, S., Mamo, D., 2003. Half a century of antipsychotics and still a central role for dopamine D2 receptors. Prog. Neuropsychopharmacol. Biol. Psychiatry 27, 1081–1090.
Kato, T., Monji, A., Hashioka, S., Kanba, S., 2007. Risperidone significantly inhibits interferon-gamma-induced microglial activation in vitro. Schizophr. Res. 92, 108–115.
Kato, T., Mizoguchi, Y., Monji, A., Horikawa, H., Suzuki, S.O., Seki, Y., Iwaki, T., Hashioka, S., Kanba, S., 2008. Inhibitory effects of aripiprazole on interferon-gamma-induced microglial activation via intracellular Ca^{2+} regulation in vitro. J. Neurochem. 106, 815–825.
Kumra, S., Ashtari, M., Cervellione, K.L., Henderson, I., Kester, H., Roofeh, D., Wu, J., Clarke, T., Thaden, E., Kane, J.M., Rhinewine, J., Lencz, T., Diamond, A., Ardekani, B.A., Szeszko, P.R., 2005. White matter abnormalities in early-onset schizophrenia: a voxel-based diffusion tensor imaging study. J. Am. Acad. Child Adolesc. Psychiatry 44, 934–941.
Lavoie, S., Murray, M.M., Deppen, P., Knyazeva, M.G., Berk, M., Boulat, O., Bovet, P., Bush, A.I., Conus, P., Copolov, D., Fornari, E., Meuli, R., Solida, A., Vianin, P., Cuenod, M., Buclin, T., Do, K.Q., 2008. Glutathione precursor, N-acetyl-cysteine, improves mismatch negativity in schizophrenia patients. Neuropsychopharmacology 33, 2187–2199.
Leucht, S., Corves, C., Arbter, D., Engel, R.R., Li, C., Davis, J.M., 2009. Second-generation versus first-generation antipsychotic drugs for schizophrenia: a meta-analysis. Lancet 373, 31–41.
Li, J., Baud, O., Vartanian, T., Volpe, J.J., Rosenberg, P.A., 2005. Peroxynitrite generated by inducible nitric oxide synthase and NADPH oxidase mediates microglial toxicity to oligodendrocytes. Proc. Natl Acad. Sci. U.S.A. 102, 9936–9941.
Liva, S.M., Kahn, M.A., Dopp, J.M., de Vellis, J., 1999. Signal transduction pathways induced by GM-CSF in microglia: significance in the control of proliferation. Glia 26, 344–352.
Merrill, J.E., Ignarro, L.J., Sherman, M.P., Melinek, J., Lane, T.E., 1993. Microglial cell cytotoxicity of oligodendrocytes is mediated through nitric oxide. J. Immunol. 151, 2132–2141.
Miyamoto, S., Duncan, G.E., Marx, C.E., Lieberman, J.A., 2005. Treatments for schizophrenia: a critical review of pharmacology and mechanisms of action of antipsychotic drugs. Mol. Psychiatry 10, 79–104.
Miyaoka, T., Yasukawa, R., Yasuda, H., Hayashida, M., Inagaki, T., Horiguchi, J., 2008. Minocycline as adjunctive therapy for schizophrenia: an open-label study. Clin. Neuropharmacol. 31, 287–292.
Mizoguchi, Y., Kanematsu, T., Hirata, M., Nabekura, J., 2003. A rapid increase in the total number of cell surface functional GABAA receptors induced by brain-derived neurotrophic factor in rat visual cortex. J. Biol. Chem. 278, 44097–44102.
Mizoguchi, Y., Monji, A., Kato, T., Seki, Y., Gotoh, L., Horikawa, H., Suzuki, S.O., Iwaki, T., Yonaha, M., Hashioka, S., Kanba, S., 2009. Brain-derived neurotrophic factor induces sustained elevation of intracellular Ca^{2+} in rodent microglia. J. Immunol. 183, 7778–7786.
Mohamed, S., Leslie, D.L., Rosenheck, R.A., 2009. Use of antipsychotics in the treatment of major depressive disorder in the U.S. Department of Veterans Affairs. J. Clin. Psychiatry 70, 906–912.
Monji, A., Kato, T., Kanba, S., 2009. Cytokines and schizophrenia: microglia hypothesis of schizophrenia. Psychiatry Clin. Neurosci. 63, 257–265.
Mortensen, P.B., Pedersen, C.B., Hougaard, D.M., Norgaard-Petersen, B., Mors, O., Borglum, A.D., Yolken, R.H., 2010. A Danish National Birth Cohort study of maternal HSV-2 antibodies as a risk factor for schizophrenia in their offspring. Schizophr. Res. 122, 257–263.
Muller, N., Krause, D., Dehning, S., Musil, R., Schennach-Wolff, R., Obermeier, M., Moller, H.J., Klauss, V., Schwarz, M.J., Riedel, M., 2010. Celecoxib treatment in an early stage of schizophrenia: results of a randomized, double-blind, placebo-controlled trial of celecoxib augmentation of amisulpride treatment. Schizophr. Res. 121, 118–124.
Ng, F., Berk, M., Dean, O., Bush, A.I., 2008. Oxidative stress in psychiatric disorders: evidence base and therapeutic implications. Int. J. Neuropsychopharmacol. 11, 851–876.
Nikodemova, M., Duncan, I.D., Watters, J.J., 2006. Minocycline exerts inhibitory effects on multiple mitogen-activated protein kinases and IkappaBalpha degradation in a stimulus-specific manner in microglia. J. Neurochem. 96, 314–323.
Park, J.S., Bateman, M.C., Goldberg, M.P., 1996. Rapid alterations in dendrite morphology during sublethal hypoxia or glutamate receptor activation. Neurobiol. Dis. 3, 215–227.
Pawate, S., Shen, Q., Fan, F., Bhat, N.R., 2004. Redox regulation of glial inflammatory response to lipopolysaccharide and interferongamma. J. Neurosci. Res. 77, 540–551.
Potkin, S.G., Saha, A.R., Kujawa, M.J., Carson, W.H., Ali, M., Stock, E., Stringfellow, J., Ingenito, G., Marder, S.R., 2003. Aripiprazole, an antipsychotic with a novel mechanism of action, and risperidone vs placebo in patients with schizophrenia and schizoaffective disorder. Arch. Gen. Psychiatry 60, 681–690.
Qian, L., Wei, S.J., Zhang, D., Hu, X., Xu, Z., Wilson, B., El-Benna, J., Hong, J.S., Flood, P.M., 2008. Potent anti-inflammatory and neuroprotective effects of TGF-beta1 are mediated through the inhibition of ERK and p47phox-Ser345 phosphorylation and translocation in microglia. J. Immunol. 181, 660–668.
Qin, L., Liu, Y., Wang, T., Wei, S.J., Block, M.L., Wilson, B., Liu, B., Hong, J.S., 2004. NADPH oxidase mediates lipopolysaccharide-induced neurotoxicity and proinflammatory gene expression in activated microglia. J. Biol. Chem. 279, 1415–1421.
Qin, B., Cartier, L., Dubois-Dauphin, M., Li, B., Serrander, L., Krause, K.H., 2006. A key role for the microglial NADPH oxidase in APP-dependent killing of neurons. Neurobiol. Aging 27, 1577–1587.
Radewicz, K., Garey, L.J., Gentleman, S.M., Reynolds, R., 2000. Increase in HLA-DR immunoreactive microglia in frontal and temporal cortex of chronic schizophrenics. J. Neuropathol. Exp. Neurol. 59, 137–150.
Salisbury, D.F., Kuroki, N., Kasai, K., Shenton, M.E., McCarley, R.W., 2007. Progressive and interrelated functional and structural evidence of post-onset brain reduction in schizophrenia. Arch. Gen. Psychiatry 64, 521–529.
Sankarapandi, S., Zweier, J.L., Mukherjee, G., Quinn, M.T., Huso, D.L., 1998. Measurement and characterization of superoxide generation in microglial cells: evidence for an NADPH oxidase-dependent pathway. Arch. Biochem. Biophys. 353, 312–321.
Sawa, A., Pletnikov, M.V., Kamiya, A., 2004. Neuron–glia interactions clarify genetic–environmental links in mental illness. Trends Neurosci. 27, 294–297.
Sawada, M., Imai, F., Suzuki, H., Hayakawa, M., Kanno, T., Nagatsu, T., 1998. Brain-specific gene expression by immortalized microglial cell-mediated gene transfer in the mammalian brain. FEBS Lett. 433, 37–40.
Schiavone, S., Sorce, S., Dubois-Dauphin, M., Jaquet, V., Colaianna, M., Zotti, M., Cuomo, V., Trabace, L., Krause, K.H., 2009. Involvement of NOX2 in the development of behavioral and pathologic alterations in isolated rats. Biol. Psychiatry 66, 384–392.
Schlosser, R.G., Nenadic, I., Wagner, G., Gullmar, D., von Consbruch, K., Kohler, S., Schultz, C.C., Koch, K., Fitzek, C., Matthews, P.M., Reichenbach, J.R., Sauer, H., 2007. White matter abnormalities and brain activation in schizophrenia: a combined DTI and fMRI study. Schizophr. Res. 89, 1–11.
Seki, Y., Suzuki, S.O., Masui, K., Harada, S., Nakamura, S., Kanba, S., Iwaki, T., in press. A simple and high-yield method for preparation of rat microglial cultures utilizing Aclar plastic film. Neuropathology. doi:10.1111/j.1440-1789.2010.01163.x. [Electronic publication ahead of print].
Seshadri, S., Kamiya, A., Yokota, Y., Prikulis, I., Kano, S., Hayashi-Takagi, A., Stanco, A., Eom, T.Y., Rao, S., Ishizuka, K., Wong, P., Korth, C., Anton, E.S., Sawa, A., 2010. Disrupted-in-Schizophrenia-1 expression is regulated by beta-site amyloid precursor protein cleaving enzyme-1-neuregulin cascade. Proc. Natl Acad. Sci. U.S.A. 107, 5622–5627.
Shapiro, D.A., Renock, S., Arrington, E., Chiodo, L.A., Liu, L.X., Sibley, D.R., Roth, B.L., Mailman, R., 2003. Aripiprazole, a novel atypical antipsychotic drug with a unique and robust pharmacology. Neuropsychopharmacology 28, 1400–1411.
Sirota, P., Gavrieli, R., Wolach, B., 2003. Overproduction of neutrophil radical oxygen species correlates with negative symptoms in schizophrenic patients: parallel studies on neutrophil chemotaxis, superoxide production and bactericidal activity. Psychiatry Res. 121, 123–132.
Steiner, J., Bielau, H., Brisch, R., Danos, P., Ullrich, O., Mawrin, C., Bernstein, H.G., Bogerts, B., 2008. Immunological aspects in the neurobiology of suicide: elevated microglial density in schizophrenia and depression is associated with suicide. J. Psychiatr. Res. 42, 151–157.
Takano, A., Arakawa, R., Ito, H., Tateno, A., Takahashi, H., Matsumoto, R., Okubo, Y., Suhara, T., 2010. Peripheral benzodiazepine receptors in patients with chronic schizophrenia: a PET study with [11C]DAA1106. Int. J. Neuropsychopharmacol. 13, 943–950.
Takeuchi, H., Mizuno, T., Zhang, G., Wang, J., Kawanokuchi, J., Kuno, R., Suzumura, A., 2005. Neuritic beading induced by activated microglia is an early feature of neuronal dysfunction toward neuronal death by inhibition of mitochondrial respiration and axonal transport. J. Biol. Chem. 280, 10444–10454.
Tan, A.S., Berridge, M.V., 2000. Superoxide produced by activated neutrophils efficiently reduces the tetrazolium salt, WST-1 to produce a soluble formazan: a simple colorimetric assay for measuring respiratory burst activation and for screening anti-inflammatory agents. J. Immunol. Methods 238, 59–68.
Treasaden, I.H., Puri, B.K., 2008. Cerebral spectroscopic and oxidative stress studies in patients with schizophrenia who have dangerously violently offended. BMC Psychiatry 8 (Suppl 1), S7.
Uranova, N.A., Vostrikov, V.M., Vikhreva, O.V., Zimina, I.S., Kolomeets, N.S., Orlovskaya, D.D., 2007. The role of oligodendrocyte pathology in schizophrenia. Int. J. Neuropsychopharmacol. 10, 537–545.
van Berckel, B.N., Bossong, M.G., Boellaard, R., Kloet, R., Schuitemaker, A., Caspers, E., Luurtsema, G., Windhorst, A.D., Cahn, W., Lammertsma, A.A., Kahn, R.S., 2008. Microglia activation in recent-onset schizophrenia: a quantitative (R)-[11C] PK11195 positron emission tomography study. Biol. Psychiatry 64, 820–822.
van Winkel, R., Stefanis, N.C., Myin-Germeys, I., 2008. Psychosocial stress and psychosis. A review of the neurobiological mechanisms and the evidence for gene–stress interaction. Schizophr. Bull. 34, 1095–1105.

Wang, J.Y., Wen, L.L., Huang, Y.N., Chen, Y.T., Ku, M.C., 2006. Dual effects of antioxidants in neurodegeneration: direct neuroprotection against oxidative stress and indirect protection via suppression of glia-mediated inflammation. Curr. Pharm. Des. 12, 3521–3533.

Wang, J.F., Shao, L., Sun, X., Young, L.T., 2009. Increased oxidative stress in the anterior cingulate cortex of subjects with bipolar disorder and schizophrenia. Bipolar Disord. 11, 523–529.

Weber, J., Lyseng-Williamson, K.A., Scott, L.J., 2008. Aripiprazole: in major depressive disorder. CNS Drugs 22, 807–813.

Yao, J.K., Reddy, R.D., van Kammen, D.P., 2001. Oxidative damage and schizophrenia: an overview of the evidence and its therapeutic implications. CNS Drugs 15, 287–310.

Yoo, A.S., McLarnon, J.G., Xu, R.L., Lee, Y.B., Krieger, C., Kim, S.U., 1996. Effects of phorbol ester on intracellular Ca^{2+} and membrane currents in cultured human microglia. Neurosci. Lett. 218, 37–40.

Zhang, X.Y., Chen da, C., Xiu, M.H., Wang, F., Qi, L.Y., Sun, H.Q., Chen, S., He, S.C., Wu, G.Y., Haile, C.N., Kosten, T.A., Lu, L., Kosten, T.R., 2009a. The novel oxidative stress marker thioredoxin is increased in first-episode schizophrenic patients. Schizophr. Res. 113, 151–157.

Zhang, X.Y., Zhou, D.F., Qi, L.Y., Chen, S., Cao, L.Y., Chen da, C., Xiu, M.H., Wang, F., Wu, G. Y., Lu, L., Kosten, T.A., Kosten, T.R., 2009b. Superoxide dismutase and cytokines in chronic patients with schizophrenia: association with psychopathology and response to antipsychotics. Psychopharmacology (Berl) 204, 177–184.

Eur Arch Psychiatry Clin Neurosci
DOI 10.1007/s00406-012-0296-9

ORIGINAL PAPER

Depressive symptoms and apathy are associated with psychomotor slowness and frontal activation

Masayo Sawa · Hidehisa Yamashita · Koichiro Fujimaki · Go Okada · Terumichi Takahashi · Shigeto Yamawaki

Received: 28 July 2011 / Accepted: 25 January 2012

Abstract Affective symptoms, such as depression and apathy, and cognitive dysfunction, such as psychomotor slowness, are known to have negative impacts on the quality of life (QOL) of patients with mental and physical diseases. However, the relationships among depressive symptoms, apathy, psychomotor slowness, and QOL in a non-clinical population are unclear. The aim of the present study was to assess these relationships and examine the underlying cortical mechanisms in a non-clinical population. Fifty-two healthy male volunteers were assessed for depressive symptoms using the Zung Self-rating Depression Scale (SDS), for apathy measured using the Apathy Scale, and QOL using the Short-Form 36 item questionnaire (SF36). The volunteers also performed the Trail Making Test Part A (TMT-A) while undergoing assessment of hemoglobin concentration changes in the frontal cortical surface using 24-channel near-infrared spectroscopy (NIRS). The scores of the SDS and Apathy Scale showed significant negative correlations with the scores of most of subscales of the SF36. In addition, the SDS score had a significant positive correlation with the time to complete the TMT-A. Further, activation of several frontal cortical areas had a significant positive correlation with the scores of the SDS and Apathy Scale. These results suggest that the degree of depressive symptoms and apathy are associated with a lower QOL in a non-clinical population and that cortical hyperactivation during a psychomotor task measured by NIRS may identify objectively individuals with a high degree of depressive symptoms and apathy.

Keywords Depressive symptoms · Apathy · Psychomotor slowness · Cortical activation · Quality of life

M. Sawa · T. Takahashi
Daijikai Mihara Hospital, 6-31-1 Nakano-cho,
Mihara, Hiroshima 723-0003, Japan

M. Sawa · H. Yamashita · G. Okada · S. Yamawaki (✉)
Department of Psychiatry and Neurosciences,
Graduate School of Biomedical Sciences, Hiroshima University,
1-2-3 Kasumi, Minami-ku, Hiroshima 734-8551, Japan
e-mail: yamawaki@hiroshima-u.ac.jp

K. Fujimaki
Department of Occupational Therapy, Faculty of Health
and Welfare, Prefectural University of Hiroshima,
1-1 Gakuen-cho, Mihara, Hiroshima 723-0053, Japan

G. Okada
Department of Psychiatry, University of Michigan,
4250 Plymouth Road, Ann Arbor, MI 8109-2700, USA

Introduction

Depressive symptoms and apathy have major impacts on the mental and physical health of individuals. Major depressive disorder (MDD), for example, is characterized by depressive symptoms and loss of interest, which is a component of apathy, and is a leading cause of worldwide disability. Worsening of depressive symptoms is associated with a reduced quality of life (QOL) [7, 17, 31]. The presence of subsyndromal depressive symptoms has also been shown to have a negative impact on psychosocial functioning [9]. In addition, there is increasing evidence that depressive symptoms are influential in the onset or progression of various kinds of diseases including Alzheimer's disease [25], coronary disease [11], and diabetes [1]. Furthermore, there is substantial evidence suggesting the negative impacts of depressive symptoms and apathy on QOL in many diseases including HIV [33], Parkinson's disease [21, 29], and brain tumors [14].

Published online: 10 February 2012

In addition to depressive symptoms and apathy, cognitive decline such as psychomotor slowness has a negative impact on social functioning of individuals. For example, Naismith et al. [20] reported that objectively measured psychomotor slowness is a significant predictor of physical disability in MDD, and Muslimovic et al. [19] reported that psychomotor slowness has a negative effect on QOL in Parkinson's disease. The Trail Making Test (TMT) is a popular neuropsychological instrument and is presumed to be a test of psychomotor skills [12, 27]. Functional neuroimaging studies have reported the involvement of the frontal cortical network in TMT [10, 18, 30, 40].

Meanwhile, neurocircuit abnormalities, an underlying condition in depressive symptoms and apathy in MDD, have been studied using neuroimaging approaches. For example, previous studies reported that anhedonic symptoms and depression severity were associated with reduced caudate volume [26] and decreased activation in the subgenual anterior cingulate cortex [16]. In addition, there is substantial evidence suggesting that psychomotor slowness in MDD is related to the fronto-striatal circuitry. Several studies using positron emission tomography (PET) reported that MDD patients with affective flattening and psychomotor slowness had decreased presynaptic dopamine function in the left caudate [2, 15].

In contrast to overt psychopathology such as MDD, there have been few studies that have examined the relationship among depressive symptoms, apathy and psychomotor slowness in a non-clinical population, and the cortical mechanisms of such symptomatology are unclear. Recently, the development of near-infrared spectroscopy (NIRS) has enabled non-invasive measurement of cortical activation under natural conditions, which enables examination while the subject performs a task related to psychomotor slowness such as the TMT-A. We hypothesized that the degree of depressive symptoms and apathy are associated with psychomotor slowness, as measured by TMT-A, and abnormal cortical activation, as measured by NIRS, as well as low QOL in a non-clinical population. We performed the following study to test this hypothesis directly.

Methods

Subjects

Fifty-two healthy male volunteers participated in this study (mean age, 37.4 ± 11.1 years). All subjects were determined to be right-handed using the Edinburgh Handedness Inventory scale [24]. Two experienced psychiatrists together excluded a participant with psychiatric symptoms above the threshold level. No subject had a history of major psychiatric disorder including major depressive disorder and anxiety disorder, neurological disorder, substance abuse, head injury, or major physical illness or was using any psychotropic medications at the time of the study. This study was approved by the Institutional Review Board of Mihara Hospital and the Prefectural University of Hiroshima. Written informed consent was obtained from each subject prior to the study.

Assessment of depressive symptoms, apathy, and QOL

Each subject was assessed for subjective depressive symptoms, extent of apathy, and QOL.

Subjective depressive symptoms were measured using the Zung Self-rating Depression Scale (SDS), a self-rating scale that consists of 20 questionnaires. The score of the SDS ranges from 20 (best) to 80 (worst), and the average is 35.1 ± 8.0 (mean ± SD) in the Japanese normal control population [5]. A higher score of the SDS is an indicative of a relatively greater degree of depressive symptoms.

Extent of apathy was measured using the Apathy Scale, a self-rating scale for assessing a tendency of apathy that consists of 16 questionnaires. The score of the Apathy Scale ranges from 0 (best) to 42 (worst), and the average is 8.7 ± 6.6 (mean ± SD) in the Japanese normal control population [23]. A higher score of the scale is an indicative of a relatively greater degree of apathy.

QOL was measured using the Medical Outcomes Study Short-Form 36-item questionnaire (SF36) [39]. SF36 is used widely to assess physical and mental well-being in social and individual contexts. Eight subscales are derived, referring to 8 health concepts: physical functioning (SF36-PF), role functioning-physical (SF36-RP), bodily pain (SF36-BP), general health (SF36-GH), vitality (SF36-VT), social functioning (SF36-SF), role functioning-emotional (SF36-RE), and mental health (SF36-MH). Each subscale ranges from 0 (worst health) to 100 (best health), and a score of 50 represents the mean score for the population.

Activation task

The activation task consisted of a 30-s pre-task baseline, a TMT-A, and a 70-s post-task baseline. Each subject sat on a comfortable chair in a quiet room, and the subject was ordered to keep their head immobile as much as possible and to not speak. During the test, the subjects were required to draw a line as rapidly as possible joining consecutive numbers (1–25), which were pseudorandomly arranged on each page. We used series of 4 TMT-A sheets, which had different circle position patterns. The time required for completing the test (TMT time) was determined as a measure of task performance. During the pre-task and

post-task periods, the subjects were instructed to draw lines repeatedly between two spots on a paper.

NIRS measurement

In this study, changes in [oxy-Hb] and [deoxy-Hb] were measured using a 24-channel NIRS machine (Hitachi ETG-100) at two wavelengths of near-infrared light (i.e., 780 and 830 nm). Absorption was measured, and [oxy-Hb] and [deoxy-Hb] were calculated. The distance between the pair of emission and detector probes was 3.0 cm, and it was considered that the machine could measure points at a depth of 2–3 cm from the scalp, that is, the surface of the cerebral cortex [8, 35]. As shown in Fig. 1, the probes of the NIRS machine were placed on the subject's bilateral frontal region. The frontal probes measured hemoglobin concentration changes at 24 measurement points in a 6 ± 15 cm area, with the lowest probes positioned along the Fp1–Fp2 line according to the international 10/20 system used in electroencephalography. The absorption of near-infrared light was measured with a time resolution of 0.1 s. The obtained data were analyzed using the ''integral mode''. The pre-task baseline was determined as the mean across the last 10 s of the 30-s pre-task period, and the post-task baseline was determined as the mean across the last 5 s of the 70-s post-task period. Linear fitting was applied to the data between these two baselines. The moving average method was used to exclude short-term motion artifacts in the analyzed data (moving average window: 5 s).

Data analyses

The analysis focused on [oxy-Hb] changes. Changes in [oxy-Hb] were assumed to more directly reflect cognitive activation than [deoxy-Hb] changes, as shown by a stronger correlation with blood-oxygenation level-dependent (BOLD) signals measured by fMRI [32].

NIRS data that clearly contained motion artifacts determined by a close observation of the subjects were excluded from analyses.

To examine the relationship among affective symptoms (SDS, Apathy Scale) and QOL (SF36), task performances (TMT time) and [oxyHb] changes during TMT, Pearson correlation analyses were conducted.

Statistical analysis was performed using PASW 18.0 software (Tokyo, Japan).

Results

Correlation between affective symptoms and QOL

Averaged scores of the SDS, Apathy Scale, and SF-36 are shown in Table 1. As shown in Table 2, the SDS negatively correlated with the SF36-RP ($r = -0.285$, $p = 0.041$), SF36-BP ($r = -0.279$, $p = 0.045$), SF36-GH ($r = -0.574$, $p < 0.001$), SF36-VT ($r = -0.635$, $p < 0.001$), SF36-RE ($r = -0.434$, $p = 0.002$), and SF36-MH ($r = -0.640$, $p < 0.001$). The Apathy Scale negatively correlated with the SF36-PF ($r = -0.367$, $p = 0.007$), SF36-GH ($r = -0.316$, $p = 0.023$), SF36-VT ($r = -0.459$, $p = 0.001$), SF36-RE ($r = -0.413$, $p = 0.002$), and SF36-MH ($r = -0.433$, $p = 0.001$). These results suggest that depressive symptoms and apathy are closely related to a lower QOL.

Correlation between affective symptoms and task performance

The average TMT time was 75.4 ± 18.3 (mean ± SD) seconds. The score of the SDS was positively correlated

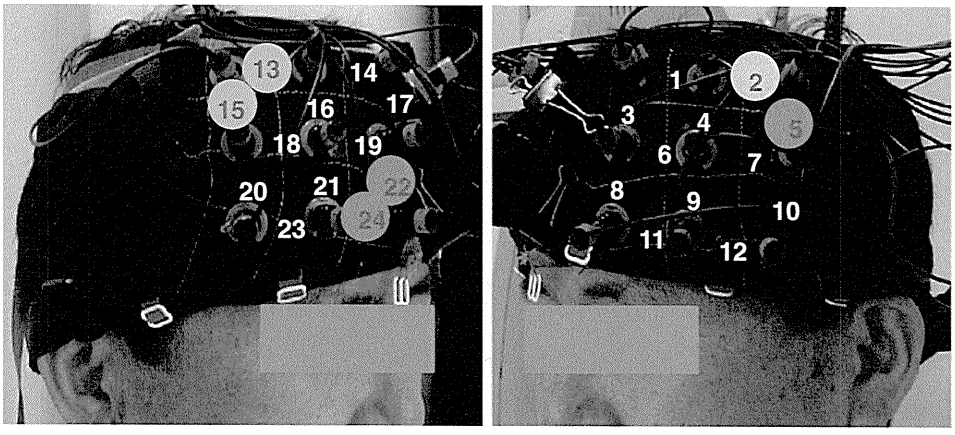

Fig. 1 Probe setting and channels showing significant correlations with the SDS and Apathy Scale. *Yellow area* indicates a channel showing significant correlations with the SDS. *Blue areas* indicate channels showing significant correlations with the Apathy Scale. *Green areas* indicate channels showing significant correlations with both the SDS and Apathy Scale

Table 1 Affective symptoms and QOL

	Mean	SD
SDS	36.8	7.7
Apathy Scale	9.8	6.0
SF36-PF	54.9	4.4
SF36-RP	50.5	7.0
SF36-BP	50.6	9.9
SF36-GH	50.9	10.9
SF36-VT	49.0	10.0
SF36-SF	50.7	8.5
SF36-RE	50.3	8.0
SF36-MH	49.4	9.2

SD standard deviation, *SDS* Zung Self-rating Depression Scale, *SF36* Medical Outcomes Study Short-Form 36-item questionnaire, *PF* physical functioning, *RP* role functioning, *BP* bodily pain, *GH* general health, *VT* vitality, *SF* social functioning, *RE* role emotional, *MH* mental health

Table 2 Correlation coefficients between affective symptoms and QOL

	SDS	Apathy Scale
SF36-PF	−0.261	−0.367**
SF36-RP	−0.285*	−0.273
SF36-BP	−0.279*	−0.207
SF36-GH	−0.574**	−0.316*
SF36-VT	−0.635**	−0.459**
SF36-SF	−0.189	−0.218
SF36-RE	−0.434**	−0.413**
SF36-MH	−0.640**	−0.433**

SDS Zung Self-rating Depression Scale, *SF36* Medical Outcomes Study Short-Form 36-item questionnaire, *PF* physical functioning, *RP* role functioning, *BP* bodily pain, *GH* general health, *VT* vitality, *SF* social functioning, *RE* role emotional, *MH* mental health

* $p < 0.05$; ** $p < 0.01$

with TMT time ($r = 0.357$, $p = 0.009$), suggesting that participants with depression took a longer time to complete the task. In contrast, there was no significant correlation between the score of the Apathy Scale and TMT time ($r = 0.261$, $p = 0.062$).

Correlation between affective symptoms and [oxy-Hb] changes during task

As shown in Table 3 and Fig. 1, [oxy-Hb] changes during the TMT-A was positively correlated with SDS in CH2 ($r = 0.442$, $p = 0.021$), CH13 ($r = 0.400$, $p = 0.013$), and CH15 ($r = 0.528$, $p = 0.006$) and with Apathy Scale in CH5 ($r = 0.451$, $p = 0.046$), CH13 ($r = 0.372$, $p = 0.021$), CH15 ($r = 0.0.711$, $p < 0.001$), CH22($r = 0.339$, $p = 0.017$), and CH24($r = 0.361$, $p = 0.009$). No channel showed [oxy-Hb] changes during the TMT-A that were negatively correlated with the SDS or the Apathy Scale. These results suggest that participants with depression and apathy required greater levels of functional activation in several brain areas to complete the task.

Table 3 Correlation coefficients between affective symptoms and [oxy-Hb] changes during TMT

Channels	SDS	Apathy Scale
1	0.38	0.28
2	0.442*	0.36
3	0.28	−0.05
4	0.09	0.09
5	0.18	0.451*
6	−0.09	0.29
7	−0.06	−0.02
8	0.21	0.19
9	−0.01	0.06
10	−0.30	0.17
11	0.11	0.22
12	−0.06	0.21
13	0.400*	0.372*
14	−0.04	−0.12
15	0.528**	0.711**
16	−0.02	0.23
17	0.12	0.22
18	−0.09	−0.01
19	0.06	0.15
20	−0.10	0.08
21	−0.14	0.07
22	0.14	0.339*
23	−0.07	0.16
24	0.06	0.361**

SDS Zung Self-rating Depression Scale

* $p < 0.05$; ** $p < 0.01$

Discussion

In this study, we demonstrated that depressive symptoms and apathy negatively affect brain function and QOL in a non-clinical population. An unexpected, but interesting result was that depressive symptoms had a greater negative impact on task performance than apathy. In this study, we showed that the score of the SDS was positively correlated with the TMT time, but the degree of apathy was not correlated with the TMT time. We also showed that participants with a high degree of depressive symptoms and apathy had a greater [oxy-Hb] increase in many frontal cortical regions.

The degree of depressive symptoms and apathy were associated with most of indices of the SF-36. Our results are consistent with those reported by McCall et al. [17], who showed that an increasing severity of depression was associated consistently with worse QOL in MDD. Our results are also consistent with those of Oguru et al. [21], who reported that both the Apathy Scale and Beck Depression Inventory scores were negatively correlated with QOL in Parkinson's disease. Together, our results suggest that the presence of depressive symptoms and apathy has a negative impact on individual QOL.

The degree of depressive symptoms was associated significantly with psychomotor slowness, but the degree of apathy was not related to psychomotor slowness. The relationship between psychomotor slowness and age has been shown in previous studies [3, 34]. In our study, age was positively correlated with the TMT time, but there was no correlation between age and affective symptoms (data not shown). Psychomotor slowness in MDD has been shown in previous studies. For example, slower response times in MDD were observed on the TMT, Rule Shift Cards, and Stroop test [6]. Our results are consistent with those reported by Rosenberg et al. [28], who showed that the Geriatric Depression Scale was associated with incident impairment on all cognitive tests including the TMT-A in healthy older women. However, our results are inconsistent with those reported by Feli et al. [4], who showed that apathy correlated with a measure of information processing speed (Stroop test B) in older MDD patients. The reason for this inconsistency is unclear, but one possible reason is a difference between the tasks for psychomotor slowness. The TMT-A may not be sufficiently sensitive to detect the effects of apathy on brain function.

We also showed that participants with high degree of depressive symptoms and apathy had a greater [oxy-Hb] increase in many frontal cortical regions. Previous neuroimaging studies on cognitive impairment in MDD have demonstrated brain activation patterns with hypo-(e.g., Okada et al. [22]) and hyper-(e.g., Walter et al. [38]) activation of frontal cortical regions [13, 37]. In such studies, performance must be taken into account before attempting interpretation, and hyperactivation in context of equal or poorer performance is usually interpreted as 'inefficiency'. In this study, we found hyperactivation in the context of equal or poorer performance with a high degree of depressive symptoms and apathy, that is, inefficiency. Our results are consistent with those of Wagner et al. [36], who reported prefrontal hyperactivation with equal performance of the Stroop test in MDD using fMRI, and with results of Walter et al. [38], who reported that prefrontal hyperactivation with poor performance of Working Memory task in MDD using fMRI. Our results suggest that participants with a high degree of depressive symptoms and apathy require greater cortical resources to perform the same task. Furthermore, lower QOL and psychomotor slowness caused by depressive symptoms and apathy may be related to such inefficient frontal activation.

Our results are inconsistent with our hypothesis. We found that apathy was associated with low QOL and frontal cortical inefficiency, but was not correlated with psychomotor slowness. One potential explanation is that the effects of apathy may be more sensitively measured by cortical [oxy-Hb] changes detected by NIRS than by behavioral output. Thus, our present methods combining behavioral and NIRS measurement enabled us to detect the effects of apathy on brain function that would be difficult to detect by behavioral output alone.

There are several limitations in this study that should be taken into consideration. First, the participants were all male because women can have potentially influential factor such as mood fluctuations across the menstrual cycle, and our findings may not be generalizable to a female population. Second, assessments of depressive symptoms and apathy are based on self-rating scales without a structured diagnostic interview (e.g., SCID). Third, age and IQ were not controlled. They are potential factors capable of affecting not only psychomotor slowness, but also brain function and QOL. Fourth, depressive symptom was measured using the SDS. Although the SDS was developed specifically for patients with a diagnosis of major depression, the SDS is commonly used even in healthy subject study, since the scale is simple and less burdensome for subjects. Fifth, power analysis and multiple comparisons were not conducted in our study as in most previous NIRS studies. Further studies should take these factors into account. With these limitations in mind, this study provides evidence to support the hypothesis that depressive symptoms and apathy were associated with psychomotor slowness and abnormal cortical activation, as well as low QOL in a non-clinical population.

In conclusion, the degree of depressive symptoms and apathy were associated with lower QOL, and participants with high degree of depressive symptoms and apathy have inefficient cortical activations. On the basis of the findings, we assume that cortical hyperactivation during a psychomotor task measured by NIRS may be used to identify objectively individuals with a high degree of depressive symptoms and apathy. Further functional neuroimaging studies focusing on depressive symptoms and apathy at a non-clinical level may elucidate the brain mechanisms underlying depressive symptoms and apathy. These studies may be beneficial for promoting the QOL of healthy subjects and patients suffering from depressive symptoms and apathy.

Acknowledgments This study is supported in part by a Grant-in-Aid from the Japanese Ministry of Health, Labour and Welfare (H21-KOKORO-general-002). The authors would like to thank S. Aoyama for helpful support of NIRS analysis.

Conflict of interest None.

References

1. Anderson RJ, Freedland KE, Clouse RE, Lustman PJ (2001) The prevalence of comorbid depression in adults with diabetes: a meta-analysis. Diabetes Care 24:1069–1078
2. Bragulat V, Paillere-Martinot ML, Artiges E, Frouin V, Poline JB, Martinot JL (2007) Dopaminergic function in depressed patients with affective flattening or with impulsivity: [18f]fluoro-l-dopa positron emission tomography study with voxel-based analysis. Psychiatry Res 154:115–124
3. Davies AD (1968) The influence of age on trail making test performance. J Clin Psychol 24:96–98
4. Feil D, Razani J, Boone K, Lesser I (2003) Apathy and cognitive performance in older adults with depression. Int J Geriatr Psychiatry 18:479–485
5. Fukuda K, Kobayashi S (1983) Sds manual, japanese version (nihon-ban sds shiyou-tebiki). Sankyodo, Kyoto
6. Gohier B, Ferracci L, Surguladze SA, Lawrence E, El Hage W, Kefi MZ, Allain P, Garre JB, Le Gall D (2009) Cognitive inhibition and working memory in unipolar depression. J Affect Disord 116:100–105
7. Gostautas A, Pranckeviciene A, Matoniene V (2006) Changes in depression and quality of life during inpatient treatment of depression. Medicina (Kaunas) 42:472–478
8. Hock C, Villringer K, Muller-Spahn F, Wenzel R, Heekeren H, Schuh-Hofer S, Hofmann M, Minoshima S, Schwaiger M, Dirnagl U, Villringer A (1997) Decrease in parietal cerebral hemoglobin oxygenation during performance of a verbal fluency task in patients with Alzheimer's disease monitored by means of near-infrared spectroscopy (NIRS)—correlation with simultaneous RCBF-pet measurements. Brain Res 755:293–303
9. Judd LL, Paulus MP, Wells KB, Rapaport MH (1996) Socioeconomic burden of subsyndromal depressive symptoms and major depression in a sample of the general population. Am J Psychiatry 153:1411–1417
10. Kubo M, Shoshi C, Kitawaki T, Takemoto R, Kinugasa K, Yoshida H, Honda C, Okamoto M (2008) Increase in prefrontal cortex blood flow during the computer version trail making test. Neuropsychobiology 58:200–210
11. Lett HS, Blumenthal JA, Babyak MA, Sherwood A, Strauman T, Robins C, Newman MF (2004) Depression as a risk factor for coronary artery disease: evidence, mechanisms, and treatment. Psychosom Med 66:305–315
12. Lezak MD, Howieson DB, Loring DW, Hannay HJ, Fischer JS (2004) Neuropsychological assessment. Oxford University Press, New York
13. Linden DE (2008) Brain imaging and psychotherapy: methodological considerations and practical implications. Eur Arch Psychiatry Clin Neurosci 258(Suppl 5):71–75
14. Mainio A, Tuunanen S, Hakko H, Niemela A, Koivukangas J, Rasanen P (2006) Decreased quality of life and depression as predictors for shorter survival among patients with low-grade gliomas: a follow-up from 1990 to 2003. Eur Arch Psychiatry Clin Neurosci 256:516–521
15. Martinot M, Bragulat V, Artiges E, Dolle F, Hinnen F, Jouvent R, Martinot J (2001) Decreased presynaptic dopamine function in the left caudate of depressed patients with affective flattening and psychomotor retardation. Am J Psychiatry 158:314–316
16. Matthews S, Simmons A, Strigo I, Gianaros P, Yang T, Paulus M (2009) Inhibition-related activity in subgenual cingulate is associated with symptom severity in major depression. Psychiatry Res 172:1–6
17. McCall WV, Cohen W, Reboussin B, Lawton P (1999) Effects of mood and age on quality of life in depressed inpatients. J Affect Disord 55:107–114
18. Moll J, de Oliveira-Souza R, Moll FT, Bramati IE, Andreiuolo PA (2002) The cerebral correlates of set-shifting: an FMRI study of the trail making test. Arq Neuropsiquiatr 60:900–905
19. Muslimovic D, Post B, Speelman JD, Schmand B, de Haan RJ (2008) Determinants of disability and quality of life in mild to moderate Parkinson disease. Neurology 70:2241–2247
20. Naismith S, Hickie I, Ward PB, Turner K, Scott E, Little C, Mitchell P, Wilhelm K, Parker G (2002) Caudate nucleus volumes and genetic determinants of homocysteine metabolism in the prediction of psychomotor speed in older persons with depression. Am J Psychiatry 159:2096–2098
21. Oguru M, Tachibana H, Toda K, Okuda B, Oka N (2010) Apathy and depression in Parkinson disease. J Geriatr Psychiatry Neurol 23:35–41
22. Okada G, Okamoto Y, Morinobu S, Yamawaki S, Yokota N (2003) Attenuated left prefrontal activation during a verbal fluency task in patients with depression. Neuropsychobiology 47:21–26
23. Okada K, Kobayashi S, Yamagata S, Takahashi K, Yamaguchi S (1997) Poststroke apathy and regional cerebral blood flow. Stroke 28:2437–2441
24. Oldfield RC (1971) The assessment and analysis of handedness: the Edinburgh inventory. Neuropsychologia 9:97–113
25. Ownby RL, Crocco E, Acevedo A, John V, Loewenstein D (2006) Depression and risk for Alzheimer disease: systematic review, meta-analysis, and metaregression analysis. Arch Gen Psychiatry 63:530–538
26. Pizzagalli DA, Holmes AJ, Dillon DG, Goetz EL, Birk JL, Bogdan R, Dougherty DD, Iosifescu DV, Rauch SL, Fava M (2009) Reduced caudate and nucleus accumbens response to rewards in unmedicated individuals with major depressive disorder. Am J Psychiatry 166:702–710
27. Reitan RM (1955) The relation of the trail making test to organic brain damage. J Consult Psychol 19:393–394
28. Rosenberg PB, Mielke MM, Xue QL, Carlson MC (2010) Depressive symptoms predict incident cognitive impairment in cognitive healthy older women. Am J Geriatr Psychiatry 18:204–211
29. Schrag A (2006) Quality of life and depression in Parkinson's disease. J Neurol Sci 248:151–157
30. Shibuya-Tayoshi S, Sumitani S, Kikuchi K, Tanaka T, Tayoshi S, Ueno S, Ohmori T (2007) Activation of the prefrontal cortex during the trail-making test detected with multichannel near-infrared spectroscopy. Psychiatry Clin Neurosci 61:616–621
31. Starkstein SE, Mayberg HS, Preziosi TJ, Andrezejewski P, Leiguarda R, Robinson RG (1992) Reliability, validity, and clinical correlates of apathy in Parkinson's disease. J Neuropsychiatry Clin Neurosci 4:134–139
32. Strangman G, Culver JP, Thompson JH, Boas DA (2002) A quantitative comparison of simultaneous bold FMRI and NIRS recordings during functional brain activation. Neuroimage 17:719–731